SCIPP 92/31
August 1992

-SCIPP-92-31-
Fermilab Library
0 1160 0011879 8

Higgs Bosons in the Minimal Supersymmetric Model: The Influence of Radiative Corrections*

HOWARD E. HABER
Santa Cruz Institute for Particle Physics
University of California, Santa Cruz, CA 95064, U.S.A.

ABSTRACT

The Higgs sector of the Minimal Supersymmetric Model (MSSM) is a CP-conserving two-Higgs doublet model that depends (at tree-level) on two Higgs parameters. In order to accurately determine the phenomenological implications of this model, one must incorporate the effects of radiative corrections. The influence of virtual Higgs exchange on precision electroweak measurements is extremely small, with the possible exception of processes involving external b and/or t quarks. On the other hand, certain natural relations of the model (such as tree-level Higgs mass relations) are substantially altered if m_t is large. Various implications of the radiatively corrected MSSM Higgs sector are explored. The theoretical upper bound to the lightest Higgs mass is determined and the influence of radiative corrections on Higgs masses and couplings is exhibited. Implications for Higgs phenomenology are briefly discussed.

To Appear in *Perspectives in Higgs Physics*,
edited by Gordon L. Kane (World Scientific, Singapore).

* Work supported in part by the U.S. Department of Energy.

Higgs Bosons in the Minimal Supersymmetric Model: The Influence of Radiative Corrections

HOWARD E. HABER
Santa Cruz Institute for Particle Physics
University of California, Santa Cruz, CA 95064, U.S.A.

ABSTRACT

The Higgs sector of the Minimal Supersymmetric Model (MSSM) is a CP-conserving two-Higgs doublet model that depends (at tree-level) on two Higgs parameters. In order to accurately determine the phenomenological implications of this model, one must incorporate the effects of radiative corrections. The influence of virtual Higgs exchange on precision electroweak measurements is extremely small, with the possible exception of processes involving external b and/or t quarks. On the other hand, certain natural relations of the model (such as tree-level Higgs mass relations) are substantially altered if m_t is large. Various implications of the radiatively corrected MSSM Higgs sector are explored. The theoretical upper bound to the lightest Higgs mass is determined and the influence of radiative corrections on Higgs masses and couplings is exhibited. Implications for Higgs phenomenology are briefly discussed.

1. Introduction

The Standard Model with minimal Higgs content is not expected to be the ultimate theoretical structure responsible for electroweak symmetry breaking [1,2]. If the Standard Model is embedded in a more fundamental structure characterized by a much larger energy scale (*e.g.*, the Planck scale, which must appear in any theory including gravity), the Higgs boson would tend to acquire mass of order the largest energy scale due to radiative corrections. Only by adjusting (*i.e.*, "fine-tuning") the parameters of the Higgs potential "unnaturally" can one arrange a large hierarchy between the Planck scale and the scale of electroweak symmetry breaking [3,4]. The Standard Model provides no mechanism for this, but supersymmetric theories have the potential to address these issues. In a supersymmetric theory the size of radiative corrections to scalar masses is controlled by the cancellation of contributions from particles and their supersymmetric partners. Since supersymmetry is not an exact symmetry of nature, the cancellation must be incomplete, and the Higgs mass receives contributions that are limited by the extent of the supersymmetry breaking. In order that the naturalness and hierarchy problems be resolved,

it is necessary that the scale of supersymmetry breaking not exceed $\mathcal{O}(1\text{ TeV})$ [5]. Such "low-energy" supersymmetric theories are especially interesting in that, to date, they provide the only theoretical framework in which the problems of naturalness and hierarchy can be resolved while retaining the Higgs bosons as truly elementary weakly coupled spin-0 particles.

The Minimal Supersymmetric extension of the Standard Model (MSSM) consists of taking the Standard Model as it is known today (including the as yet undiscovered t-quark) and adding the corresponding supersymmetric partners [6,7]. In addition, the MSSM must possess two Higgs doublets in order to give masses to up and down type fermions in a manner consistent with supersymmetry (and to avoid gauge anomalies introduced by the fermionic superpartners of the Higgs bosons). In particular, the MSSM Higgs sector is a CP-conserving two-Higgs-doublet model, which can be parametrized at tree-level in terms of two Higgs sector parameters. This structure arises due to constraints imposed by supersymmetry that determine the Higgs quartic couplings in terms of electroweak gauge coupling constants.

In section 2, I review the general structure of the (nonsupersymmetric) two-Higgs-doublet extension of the Standard Model. By imposing the constraints of supersymmetry on the quartic terms of the Higgs potential (and the Higgs-fermion interaction) one obtains the Higgs sector of the MSSM. The tree-level predictions of this model are briefly summarized in section 3. In section 4, I investigate the size of Higgs-induced radiative corrections to electroweak processes. Higgs radiative corrections that enter through the correction to gauge boson propagators are extremely small. On the other hand, virtual Higgs effects in processes involving external b and/or t quarks may be large enough to be observable. The most dramatic effect of radiative corrections to the MSSM Higgs sector is the modification of tree-level mass relations of the model. Section 5 demonstrates that the tree-level bound restricting the lightest CP-even Higgs scalar to be lighter than the Z can be significantly violated if the top quark mass is large. Radiative corrections to MSSM Higgs masses and couplings in the leading logarithmic approximation are described in section 6 and some numerical results for Higgs masses are presented in section 7. Finally, some implications of the radiatively-corrected Higgs sector are explored in section 8. Certain technical details are relegated to three appendices.

2. The Two-Higgs Doublet Model

I begin with a brief review of the general (non-supersymmetric) two-Higgs doublet extension of the Standard Model [8]. Let Φ_1 and Φ_2 denote two complex $Y = 1$, $\mathrm{SU}(2)_L$ doublet scalar fields. The most general gauge invariant scalar

potential is given by

$$\begin{aligned}\mathcal{V} = {} & m_{11}^2\Phi_1^\dagger\Phi_1 + m_{22}^2\Phi_2^\dagger\Phi_2 - [m_{12}^2\Phi_1^\dagger\Phi_2 + \text{h.c.}] \\ & + \tfrac{1}{2}\lambda_1(\Phi_1^\dagger\Phi_1)^2 + \tfrac{1}{2}\lambda_2(\Phi_2^\dagger\Phi_2)^2 + \lambda_3(\Phi_1^\dagger\Phi_1)(\Phi_2^\dagger\Phi_2) + \lambda_4(\Phi_1^\dagger\Phi_2)(\Phi_2^\dagger\Phi_1) \\ & + \left\{\tfrac{1}{2}\lambda_5(\Phi_1^\dagger\Phi_2)^2 + [\lambda_6(\Phi_1^\dagger\Phi_1) + \lambda_7(\Phi_2^\dagger\Phi_2)]\Phi_1^\dagger\Phi_2 + \text{h.c.}\right\}.\end{aligned} \tag{1}$$

In most discussions of two-Higgs-doublet models, the terms proportional to λ_6 and λ_7 are absent. This can be achieved by imposing a discrete symmetry $\Phi_1 \to -\Phi_1$ on the model. Such a symmetry would also require $m_{12} = 0$ unless we allow a soft violation of this discrete symmetry by dimension-two terms.* For the moment, I will refrain from setting any of the coefficients in eq. (1) to zero. In principle, m_{12}^2, λ_5, λ_6 and λ_7 can be complex. However, I shall ignore the possibility of CP-violating effects in the Higgs sector by choosing all coefficients in eq. (1) to be real. The scalar fields will develop non-zero vacuum expectation values if the mass matrix m_{ij}^2 has at least one negative eigenvalue. Imposing CP invariance and $\mathrm{U(1)_{EM}}$ gauge symmetry, the minimum of the potential is

$$\langle\Phi_1\rangle = \frac{1}{\sqrt{2}}\begin{pmatrix}0\\ v_1\end{pmatrix}, \qquad \langle\Phi_2\rangle = \frac{1}{\sqrt{2}}\begin{pmatrix}0\\ v_2\end{pmatrix}, \tag{2}$$

where the v_i can be chosen to be real. It is convenient to introduce the following notation:

$$v^2 \equiv v_1^2 + v_2^2 = \frac{4m_W^2}{g^2}, \qquad t_\beta \equiv \tan\beta \equiv \frac{v_2}{v_1}. \tag{3}$$

Of the original eight scalar degrees of freedom, three Goldstone bosons ($G^\pm$ and G^0) are absorbed ("eaten") by the $W^\pm$ and Z. The remaining five physical Higgs particles are: two CP-even scalars (h^0 and H^0, with $m_{h^0} \le m_{H^0}$), one CP-odd scalar (A^0) and a charged Higgs pair ($H^\pm$). The mass parameters m_{11} and m_{22} can be eliminated by minimizing the scalar potential. The resulting squared masses for the CP-odd and charged Higgs states are

$$\begin{aligned} m_{A^0}^2 &= \frac{m_{12}^2}{s_\beta c_\beta} - \tfrac{1}{2}v^2\left(2\lambda_5 + \lambda_6 t_\beta^{-1} + \lambda_7 t_\beta\right), \\ m_{H^\pm}^2 &= m_{A^0}^2 + \tfrac{1}{2}v^2(\lambda_5 - \lambda_4). \end{aligned} \tag{4}$$

* This latter requirement is sufficient to guarantee the absence of Higgs-mediated tree-level flavor changing neutral currents.

The two CP-even Higgs states mix according to the following squared mass matrix:

$$\begin{aligned}\mathcal{M}^2 = {} & m_{A^0}^2\begin{pmatrix} s_\beta^2 & -s_\beta c_\beta \\ -s_\beta c_\beta & c_\beta^2\end{pmatrix} \\ & + v^2\begin{pmatrix} \lambda_1 c_\beta^2 + 2\lambda_6 s_\beta c_\beta + \lambda_5 s_\beta^2 & (\lambda_3+\lambda_4)s_\beta c_\beta + \lambda_6 c_\beta^2 + \lambda_7 s_\beta^2 \\ (\lambda_3+\lambda_4)s_\beta c_\beta + \lambda_6 c_\beta^2 + \lambda_7 s_\beta^2 & \lambda_2 s_\beta^2 + 2\lambda_7 s_\beta c_\beta + \lambda_5 c_\beta^2\end{pmatrix},\end{aligned} \tag{5}$$

where $s_\beta \equiv \sin\beta$ and $c_\beta \equiv \cos\beta$. The physical mass eigenstates are

$$\begin{aligned} H^0 &= (\sqrt{2}\mathrm{Re}\,\Phi_1^0 - v_1)\cos\alpha + (\sqrt{2}\mathrm{Re}\,\Phi_2^0 - v_2)\sin\alpha, \\ h^0 &= -(\sqrt{2}\mathrm{Re}\,\Phi_1^0 - v_1)\sin\alpha + (\sqrt{2}\mathrm{Re}\,\Phi_2^0 - v_2)\cos\alpha. \end{aligned} \tag{6}$$

The corresponding masses are

$$m_{H^0,h^0}^2 = \tfrac{1}{2}\left[\mathcal{M}_{11}^2 + \mathcal{M}_{22}^2 \pm \sqrt{(\mathcal{M}_{11}^2 - \mathcal{M}_{22}^2)^2 + 4(\mathcal{M}_{12}^2)^2}\right], \tag{7}$$

and the mixing angle α is obtained from

$$\begin{aligned} \sin 2\alpha &= \frac{2\mathcal{M}_{12}^2}{\sqrt{(\mathcal{M}_{11}^2 - \mathcal{M}_{22}^2)^2 + 4(\mathcal{M}_{12}^2)^2}}, \\ \cos 2\alpha &= \frac{\mathcal{M}_{11}^2 - \mathcal{M}_{22}^2}{\sqrt{(\mathcal{M}_{11}^2 - \mathcal{M}_{22}^2)^2 + 4(\mathcal{M}_{12}^2)^2}}. \end{aligned} \tag{8}$$

The phenomenology of the two-Higgs doublet model depends in detail on the various couplings of the Higgs bosons to gauge bosons, Higgs bosons and fermions. The Higgs couplings to gauge bosons follow from gauge invariance and are thus model independent. For example, using the symbol ϕ^0 for the minimal Higgs boson of the Standard Model, the couplings of the two CP-even Higgs bosons to W and Z pairs are given in terms of the angles α and β by

$$\begin{aligned} g_{h^0VV} &= g_{\phi^0VV}\sin(\beta-\alpha) \\ g_{H^0VV} &= g_{\phi^0VV}\cos(\beta-\alpha), \end{aligned} \tag{9}$$

where $g_{\phi^0VV} \equiv g_V m_V$ and

$$g_V = \begin{cases} g, & V = W, \\ g/\cos\theta_W, & V = Z. \end{cases} \tag{10}$$

There are no tree-level couplings of A^0 or $H^\pm$ to VV. Gauge invariance also determines the strength of the trilinear couplings of one gauge boson to two Higgs

bosons. For example,

$$g_{h^0A^0Z} = \frac{g\cos(\beta-\alpha)}{2\cos\theta_W}, \qquad g_{H^0A^0Z} = \frac{-g\sin(\beta-\alpha)}{2\cos\theta_W}. \tag{11}$$

In the examples shown above, some of the couplings can be suppressed if either $\sin(\beta-\alpha)$ or $\cos(\beta-\alpha)$ is very small. If the theory yields a Higgs mass spectrum in which the h^0 is considerably lighter than the other physical Higgs scalars, then the h^0 couplings will typically approach their Standard Model values [9]. In this limit, $\cos(\beta-\alpha) \to 0$. More generally, all the Higgs couplings cannot vanish simultaneously. From the expressions above, we see that the following sum rules must hold separately for $V = W$ and Z:

$$g^2_{H^0VV} + g^2_{h^0VV} = g^2_{\phi^0VV}, \qquad g^2_{h^0A^0Z} + g^2_{H^0A^0Z} = \frac{g^2}{4\cos^2\theta_W}. \tag{12}$$

These results are a consequence of the tree-unitarity of the electroweak theory [10]. Moreover, if we focus on a given CP-even Higgs state, we note that its couplings to VV and A^0V cannot be simultaneously suppressed, since eqs. (9)–(11) imply that

$$g^2_{hZZ} + 4m_Z^2 g^2_{hA^0Z} = \frac{g^2m_Z^2}{\cos^2\theta_W}, \tag{13}$$

for $h = h^0$ or H^0. Similar considerations also hold for the coupling of h^0 and H^0 to $W^\pm H^\mp$. We can summarize the above results by noting that the coupling of h^0 and H^0 to vector boson pairs or vector–scalar boson final states is proportional to either $\sin(\beta-\alpha)$ or $\cos(\beta-\alpha)$ as indicated below.

$\cos(\beta-\alpha)$	$\sin(\beta-\alpha)$
$H^0W^+W^-$	$h^0W^+W^-$
H^0ZZ	h^0ZZ
ZA^0h^0	ZA^0H^0
$W^\pm H^\mp h^0$	$W^\pm H^\mp H^0$

(14)

The 3-point and 4-point Higgs self-couplings depend on the parameters of the two-Higgs-doublet potential [eq. (1)]. The Feynman rules for the trilinear Higgs vertices are listed in Appendix A. The Feynman rules for the 4-point Higgs vertices are rather tedious in the general two-Higgs-doublet model and will not be given here.

The Higgs couplings to fermions are model dependent, although their form is often constrained by discrete symmetries that are imposed in order to avoid tree-level flavor changing neutral currents mediated by Higgs exchange [11]. An example of a model that respects this constraint is one in which one Higgs doublet (before symmetry breaking) couples exclusively to down-type fermions and the other Higgs doublet couples exclusively to up-type fermions. This is the pattern of couplings found in the minimal supersymmetric model (MSSM). The results in this case are as follows. The couplings of the neutral Higgs bosons to $f\bar{f}$ relative to the Standard Model value, $gm_f/2m_W$, are given by (using 3rd family notation)

$$\begin{array}{llll} H^0t\bar{t}: & \dfrac{\sin\alpha}{\sin\beta} & H^0b\bar{b}: & \dfrac{\cos\alpha}{\cos\beta} \\ h^0t\bar{t}: & \dfrac{\cos\alpha}{\sin\beta} & h^0b\bar{b}: & \dfrac{-\sin\alpha}{\cos\beta} \\ A^0t\bar{t}: & \gamma_5\cot\beta & A^0b\bar{b}: & \gamma_5\tan\beta, \end{array} \tag{15}$$

(the γ_5 indicates a pseudoscalar coupling), and the charged Higgs boson coupling is given by

$$g_{H^-t\bar{b}} = \frac{g}{2\sqrt{2}m_W}\,[m_t\cot\beta(1+\gamma_5) + m_b\tan\beta(1-\gamma_5)]. \tag{16}$$

Finally, consider the experimental constraints on the parameters of the two-Higgs doublet model. Limits on the charged and neutral Higgs masses have been obtained at LEP. Here I briefly summarize the results for the Higgs search as compiled by the Particle Data Group [12]. For the charged Higgs boson, $m_{H^\pm} >$ 41.7 GeV. This is the most model independent bound and assumes only that the $H^\pm$ decays dominantly into $\tau^+\nu_\tau$, $c\bar{s}$ and $c\bar{b}$. The LEP limits on the masses of h^0 and A^0 are obtained by searching simultaneously for $Z \to h^0f\bar{f}$ and $Z \to h^0A^0$ [13,14]. The ZZh^0 and Zh^0A^0 couplings that govern these two decay rates are proportional to $\sin(\beta-\alpha)$ and $\cos(\beta-\alpha)$, respectively. Thus, one can use the LEP data to deduce limits on m_{h^0} and m_{A^0} as a function of $\sin(\beta-\alpha)$. Stronger limits can be obtained in the MSSM where $\sin(\beta-\alpha)$ is fixed by other model parameters. The present limits as summarized by the Particle Data Group [12] are $m_{h^0} > 29$ GeV and $m_{A^0} > 12$ GeV based on supersymmetric tree-level relations among Higgs parameters, but with no assumption for the value of $\tan\beta$. If leading log radiative corrections are incorporated and $\tan\beta > 1$ is assumed, then recent results of the ALEPH Collaboration [14] yield $m_{h^0} > 41$ GeV and $m_{A^0} > 20$ GeV (at 95% CL). However, the limit on m_{h^0} may be substantially weaker if large squark mixing is permitted [15].

The experimental information on the parameter $\tan\beta$ is quite meager. For definiteness, let us assume that the Higgs-fermion couplings are specified as in the MSSM. In the Standard Model, the Higgs coupling to top quarks is proportional to $gm_t/2m_W$, and is therefore the strongest of all Higgs-fermion couplings. For $\tan\beta < 1$, the Higgs couplings to top-quarks in the two-Higgs-doublet model discussed above are further enhanced by a factor of $1/\tan\beta$. As a result, some weak experimental limits on $\tan\beta$ exist based on the non-observation of virtual effects involving the $H^-t\bar{b}$ coupling. Clearly, such limits depend both on $m_{H^\pm}$ and $\tan\beta$. For example, for $m_{H^\pm} \simeq m_W$, limits from the analysis of B^0-$\overline{B^0}$ mixing imply that $\tan\beta \gtrsim 0.5$ [16]. No comparable limits exist based on top-quark couplings to neutral Higgs bosons.

Theoretical constraints on $\tan\beta$ are also useful. If $\tan\beta$ becomes too small, then the Higgs coupling to top quarks becomes strong. In this case, the tree-unitarity of processes involving the Higgs-top quark Yukawa coupling is violated. Perhaps this should not be regarded as a theoretical defect, although it does render any perturbative analysis unreliable. A rough lower bound advocated by ref. 16, $\tan\beta \gtrsim m_t/600$ GeV, corresponds to a Higgs-top quark coupling in the perturbative region. A similar argument involving the Higgs-bottom quark coupling would yield $\tan\beta \lesssim 120$. A more solid theoretical constraint is based on the requirement that Higgs-fermion couplings remain finite when running from the electroweak scale to some large energy scale Λ [17–19]. Beyond Λ, one assumes that new physics enters. The limits on $\tan\beta$ depend on m_t and the choice of the high energy scale Λ. Using the renormalization group equations given in Appendix B, we integrate from the electroweak scale to Λ (allowing for the possible existence of a supersymmetry-breaking scale, $m_Z \leq M_{\rm SUSY} \leq \Lambda$), and determine the region of $\tan\beta$–m_t parameter space in which the Higgs-fermion Yukawa couplings remain finite. (The t, b and τ are all included in the analysis.) The results are shown in figs. 1 and 2 for two different choices of Λ [19]. The allowed region of parameter space lies below the curves shown. For example, if there is no new physics (other than perhaps minimal supersymmetry) below the grand unification scale of 10^{16} GeV, then based on the CDF limit [20] of $m_t > 91$ GeV, one would conclude that $0.5 \lesssim \tan\beta \lesssim 50$. The lower limit on $\tan\beta$ becomes even sharper if the top-quark mass is heavier. Remarkably, the limits on $\tan\beta$ do not get substantially weaker for Λ as low as 100 TeV. Finally, it is interesting to note that the limits on $\tan\beta$ shown in fig. 2 are not very different from those that emerge from models of low-energy supersymmetry based on supergravity which strongly favor $\tan\beta > 1$ [21].

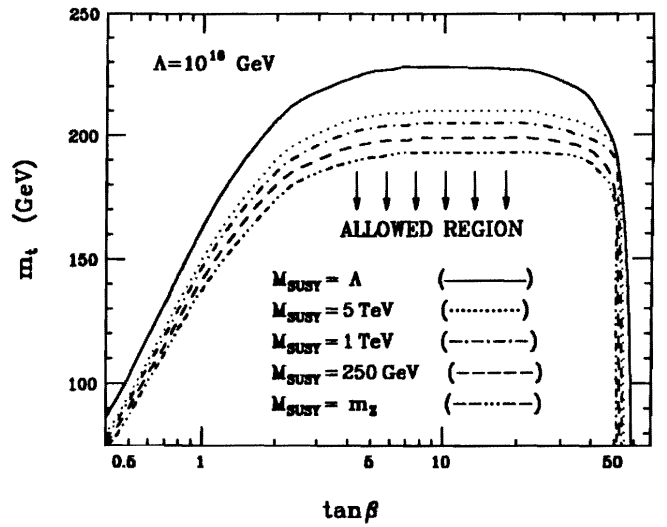

Fig. 1. The region of $\tan\beta$–m_t parameter space in which all running Higgs-fermion Yukawa couplings remain finite at all energy scales, μ, from m_Z to $\Lambda = 10^{16}$ GeV [19]. Non-supersymmetric two-Higgs-doublet (one-loop) renormalization group equations (RGEs) are used for $m_Z \leq \mu \leq M_{\rm SUSY}$ and the RGEs of the minimal supersymmetric model are used for $M_{\rm SUSY} \leq \mu \leq \Lambda$ (see Appendix B). Five different values of $M_{\rm SUSY}$ are shown; the allowed parameter space lies below the respective curves.

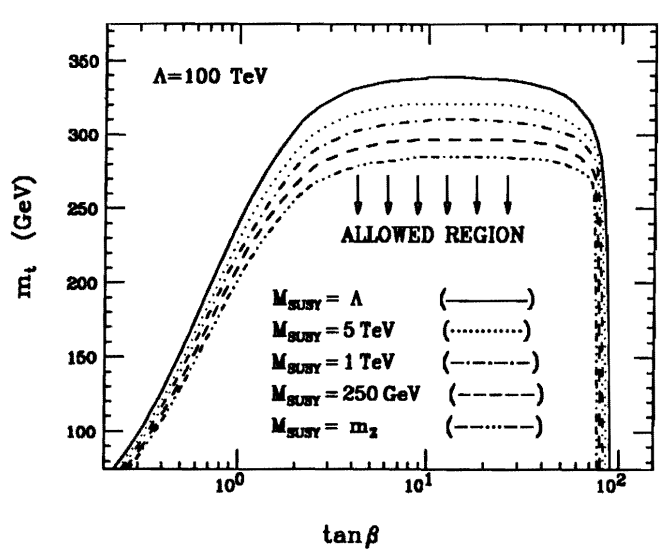

Fig. 2. The region of $\tan\beta$–m_t parameter space in which all running Higgs-fermion Yukawa couplings remain finite at all energy scales from m_Z to $\Lambda = 100$ TeV. See caption to fig. 1.

3. The Higgs Sector of the MSSM at Tree Level

The Higgs sector of the MSSM is a CP-conserving two-Higgs-doublet model, with a Higgs potential whose dimension-four terms respect supersymmetry and with restricted Higgs-fermion couplings in which Φ_1 couples exclusively to down-type fermions while Φ_2 couples exclusively to up-type fermions [8]. Using the notation of eq. (1), the quartic couplings λ_i are given by

$$\begin{aligned} \lambda_1 &= \lambda_2 = \tfrac{1}{4}(g^2 + g'^2)\,, \\ \lambda_3 &= \tfrac{1}{4}(g^2 - g'^2)\,, \\ \lambda_4 &= -\tfrac{1}{2}g^2\,, \\ \lambda_5 &= \lambda_6 = \lambda_7 = 0\,. \end{aligned} \tag{17}$$

Inserting these results into eqs. (4) and (5), it follows that

$$\begin{aligned} m^2_{A^0} &= m^2_{12}(\tan\beta + \cot\beta)\,, \\ m^2_{H^\pm} &= m^2_{A^0} + m^2_W\,, \end{aligned} \tag{18}$$

and the neutral CP-even mass matrix is given by

$$\mathcal{M}^2 = \begin{pmatrix} m^2_{A^0}\sin^2\beta + m^2_Z\cos^2\beta & -(m^2_{A^0} + m^2_Z)\sin\beta\cos\beta \\ -(m^2_{A^0} + m^2_Z)\sin\beta\cos\beta & m^2_{A^0}\cos^2\beta + m^2_Z\sin^2\beta \end{pmatrix}. \tag{19}$$

The eigenvalues of $\mathcal{M}^2$ are the squared masses of the two CP-even Higgs scalars

$$m^2_{H^0,h^0} = \tfrac{1}{2}\left(m^2_{A^0} + m^2_Z \pm \sqrt{(m^2_{A^0} + m^2_Z)^2 - 4m^2_Z m^2_{A^0}\cos^2 2\beta}\right). \tag{20}$$

and the diagonalizing angle is α, with

$$\cos 2\alpha = -\cos 2\beta\left(\frac{m^2_{A^0} - m^2_Z}{m^2_{H^0} - m^2_{h^0}}\right), \qquad \sin 2\alpha = -\sin 2\beta\left(\frac{m^2_{H^0} + m^2_{h^0}}{m^2_{H^0} - m^2_{h^0}}\right). \tag{21}$$

From the expressions for the Higgs masses obtained above, the following inequalities are easily established

$$\begin{aligned} & m_{h^0} \le m_{A^0} \\ & m_{h^0} \le m|\cos 2\beta| \le m_Z\,, \qquad \text{with } m \equiv min(m_Z, m_{A^0}) \\ & m_{H^0} \ge m_Z\,, \\ & m_{H^\pm} \ge m_W\,. \end{aligned} \tag{22}$$

Thus, in the MSSM, two parameters (conveniently chosen to be m_{A^0} and $\tan\beta$) suffice to fix all other tree-level Higgs sector parameters.

4. Virtual Higgs Contributions to Precision Electroweak Measurements

After three years of running at LEP and more than two million Z^0 events accumulated, the Standard Model of particle physics continues to provide a detailed and accurate description of all observed high energy physics phenomena. In particular, precision measurements of various electroweak observables are now possible that are sensitive to one-loop predictions of the theory. Apart from providing very sensitive tests of the Standard Model, such measurements can impose severe constraints on theories that incorporate physics beyond the Standard Model.

The Standard Model is usually assumed to be an effective low-energy limit of a more fundamental theory. Let M be the minimum characteristic energy scale at which new physics beyond the Standard Model enters. For example, theoretical attempts to address the hierarchy and naturalness problems (see section 1) usually take M no larger than about 1 TeV. We then can pose the following question. Can evidence of physics at the scale M be detected through its virtual corrections to electroweak observables? In order to address this question, one must first determine the expected size of such radiative corrections. The decoupling theorem [22] implies that radiative corrections to electroweak observables from such new physics should be of $\mathcal{O}(g^2 m^2_Z/M^2)$. That is, the virtual effects due to new physics formally decouple as $M \to \infty$. However, in spontaneously broken gauge theories, an exception to the decoupling theorem arises [23-25]. Suppose we wish to consider the virtual effects of a certain particle whose mass m is proportional to a dimensionless coupling of the theory. In this case, the virtual effects due to such a particle do *not* decouple in the large m limit. Two examples in the Standard Model are the top quark, whose mass is proportional to a Higgs-quark Yukawa coupling, and the Higgs boson, whose mass is proportional to the Higgs self-coupling.

The classic example of non-decoupling can be seen in the ρ-parameter of electroweak physics [23,26]. If one defines $\rho \equiv m^2_W/m^2_Z\cos^2\theta_W$, then at tree-level $\rho = 1$ in any SU(2)×U(1) model whose Higgs sector consists entirely of weak scalar doublets (*e.g.*, the Standard Model and the MSSM). Since $\rho = 1$ is a "natural" relation in such models, the deviation of ρ from one is calculable when radiative corrections are incorporated. To proceed, one must carefully define the observables of the model in order to establish a useful one-loop definition for ρ. For example, in ref. 27, $\rho \equiv \rho_{NC}$ is defined as the renormalization factor in the one-loop neutral current neutrino-nucleon scattering amplitudes when expressed in terms of the Fermi constant G_F. A recent theoretical analysis of LEP data in ref. 28 gives $\rho = 0.9995 \pm 0.0051$. In the Standard Model, the deviation of ρ from 1 is predicted to be quite small unless there exist particles with nontrivial electroweak quantum numbers that are substantially heavier than the Z boson. It is therefore convenient to define

$$\rho \equiv \rho_{\rm RSM} + \delta\rho\,, \tag{23}$$

where $\rho_{\rm RSM} \simeq 1$ is the ρ parameter in a "reference Standard Model" (RSM) in which the radiative corrections to ρ are very small. In order to exhibit the explicit dependence of ρ on the top quark and Higgs masses, let us choose a RSM in which $m_t = m_b$ and $m_{\phi^0} = m_Z$ (where m_{ϕ^0} is the mass of the Standard Model Higgs boson). Then, in the Standard Model, assuming $m_{\phi^0} \gg m_Z$ [23,26,27]

$$\begin{aligned}\delta\rho \simeq \frac{g^2 N_c}{64\pi^2 m_W^2}\left[m_t^2 + m_b^2 - \frac{2m_t^2 m_b^2}{m_t^2 - m_b^2}\ln\left(\frac{m_t^2}{m_b^2}\right)\right] \\ - \frac{3g^2}{64\pi^2 c_W^2}\left[s_W^2 \ln\left(\frac{m_{\phi^0}^2}{m_Z^2}\right) - \frac{c_W^4}{s_W^2}\ln\left(\frac{m_W^2}{m_Z^2}\right) - 1\right],\end{aligned} \tag{24}$$

where $N_c = 3$, $s_W \equiv \sin\theta_W$ and $c_W \equiv \cos\theta_W$. m_{ϕ^0} is assumed to be much larger than m_Z. As advertised, the decoupling theorem is not respected in the limit of large top quark and/or Higgs mass. The quadratic dependence of $\delta\rho$ on m_t yields a useful constraint on the top quark mass.* In contrast, the dependence of $\delta\rho$ on Higgs mass is only logarithmic and is therefore not very useful in constraining the Higgs mass.†

The contributions of physics beyond the Standard Model to electroweak observables occur primarily through virtual loop corrections to gauge boson propagators, sometimes called "oblique" corrections [32]. This is often a good approximation when it comes to the study of virtual Higgs boson corrections, since the Higgs coupling to light fermions is suppressed by a factor m_f/m_W. However, there are a number of cases where one-loop vertex and box corrections involving the coupling of charged Higgs bosons to $t\bar{b}$ can lead to interesting effects. I will return to this possibility at the end of this section. For the moment, I shall work in the oblique approximation and assume that the radiative corrections to an electroweak observable of interest are dominated by virtual heavy particle corrections to gauge boson propagators.

In the limit where the heavy particle masses are much larger than the Z mass, the heavy particle contributions to oblique radiative corrections can be summarized in terms of three numbers called S, T and U [33-36]. T is related simply to the ρ parameter

$$\rho - 1 = \alpha T, \tag{25}$$

where α is the usual fine structure constant. To formally define the three quantities

* Radiative corrections to other electroweak observables also depend nontrivially on m_t (*e.g.*, see refs. [28-30]). A comprehensive analysis of electroweak data quoted in the 1992 Particle Data Group compilation [12] yields $m_t < 201$ GeV at 95% CL.

† This is an example of Veltman's screening theorem [31].

S, T and U, one proceeds as follows. Let

$$i\Pi_{ij}^{\mu\nu}(q) = ig^{\mu\nu}A_{ij}(q^2) + iq^\mu q^\nu B_{ij}(q^2), \tag{26}$$

be equal to the sum of all one-loop Feynman graphs contributing to the V_i–V_j two-point function, where q is the four-momentum of the vector boson ($V = W$, Z or γ). Only the functions A_{ij} are relevant for the subsequent analysis. It is convenient to write

$$A_{ij}(q^2) = A_{ij}(0) + q^2 F_{ij}(q^2), \tag{27}$$

which define the quantities F_{ij}. Gauge invariance implies that $A_{\gamma\gamma}(0) = 0$.‡ A major simplification takes place if one is interested in the effects of "heavy" physics (characterized by a scale $M \gg m_Z$) on electroweak observables. In this case, since q^2 is of order m_Z^2, one only makes an error of $\mathcal{O}(m_Z^2/M^2)$ by neglecting the q^2 dependence of the F_{ij}. Then, one can show that the oblique corrections to electroweak observables due to heavy physics can be expressed in terms of three particular combinations of the $A_{ij}(0)$ and F_{ij}

$$\begin{aligned}\alpha T &\equiv \frac{A_{WW}(0)}{m_W^2} - \frac{A_{ZZ}(0)}{m_Z^2} - \frac{2s_W}{c_W}\frac{A_{Z\gamma}(0)}{m_Z^2} \\ \frac{g^2}{16\pi c_W^2}S &\equiv F_{ZZ}(m_Z^2) - F_{\gamma\gamma}(m_Z^2) + \left(\frac{2s_W^2 - 1}{s_W c_W}\right)F_{Z\gamma}(m_Z^2) \\ \frac{g^2}{16\pi}(S+U) &\equiv F_{WW}(m_W^2) - F_{\gamma\gamma}(m_W^2) - \frac{c_W}{s_W}F_{Z\gamma}(m_W^2).\end{aligned} \tag{28}$$

Note that the $A_{ij}(0)$ and F_{ij} in the above formulae are divergent quantities. Nevertheless, if one includes a complete set of contributions from a gauge invariant sector, then S, T, and U will be finite constants. The Higgs sector by itself does not constitute a gauge invariant sector in this regard, so one must include the vector boson sector as well to obtain a non-divergent result for S, T and U. Alternatively, in order to obtain finite quantities that solely reflect the influence of heavy Higgs physics, one can define δS, δT and δU relative to some reference Standard Model where m_{ϕ^0} is fixed to a convenient value. For example, if we choose a RSM with $m_{\phi^0} = m_Z$, then the change in S due to a fourth generation of fermions U and D (with electric charges $e_D + 1$ and e_D respectively) and a heavy Higgs boson of

‡ In addition, the sum of heavy particle contributions to $A_{Z\gamma}(0)$ also vanishes exactly. Only gauge boson loops can produce nonzero contributions to $A_{Z\gamma}(0)$ (in the standard R-gauge).

mass m_{ϕ^0} is given by

$$\delta S \simeq \frac{N_c}{6\pi}\left[1+(1+2e_D)\ln\left(\frac{m_D^2}{m_U^2}\right)\right]+\frac{1}{12\pi}\left[\ln\left(\frac{m_{\phi^0}^2}{m_Z^2}\right)-3\pi\sqrt{3}+\frac{107}{6}\right], \quad (29)$$

where m_U, m_D, $m_{\phi^0} \gg m_Z$ has been assumed. Once again, the non-decoupling effects of the heavy physics are apparent.

Radiative corrections (in the oblique approximation) to electroweak observables can be expressed in terms of S, T and U. The ρ-parameter discussed above is one such example. A second example is the W mass prediction. The one-loop prediction is obtained by solving the following equation for the W mass

$$m_W^2\left(1-\frac{m_W^2}{m_Z^2}\right)=\left(\frac{\pi\alpha}{\sqrt{2}G_F}\right)^2\frac{1}{1-\Delta r}, \quad (30)$$

where $\pi\alpha/\sqrt{2}G_F = (37.2802\ \text{GeV})^2$ and

$$\Delta r = \frac{g^2}{8\pi}\left[S-2c_W^2T+\left(\frac{2s_W^2-1}{2s_W^2}\right)U\right]. \quad (31)$$

Other examples can be found in refs. 33-35. Thus the effects of heavy physics on numerous electroweak observables are immediately known once the corresponding contributions to S, T and U have been computed.

In order to compute the contributions of the Higgs sector of the MSSM to S, T and U one must first define the RSM. Then,

$$\begin{aligned} S &= S_{\text{RSM}}+\delta S, \\ T &= T_{\text{RSM}}+\delta T, \\ U &= U_{\text{RSM}}+\delta U, \end{aligned} \quad (32)$$

where the MSSM Higgs sector contributions to δS, δT and δU are obtained from eq. (28) by computing the MSSM Higgs loops contributing to $A_{ij}(0)$ and F_{ij} (including diagrams with one virtual Higgs boson and one virtual gauge boson) and subtracting off the corresponding Higgs loops to the RSM. In nearly all cases of interest, one finds that $\delta U \ll \delta S$, δT, so I shall focus on δS and δT below. In the present case, it is most convenient to define the RSM to be the Standard Model with the Standard Model Higgs boson mass set equal to the mass of the lightest CP-even Higgs boson of the MSSM. In addition, until m_t is known, the definitions

of δS and δT will depend on the value of m_t chosen for the RSM. Typically, one chooses $m_t = m_Z$ (equal to the present experimental CDF lower bound [20]) in order to obtain conservative limits on the possible new physics contributions to S and T.

Consider now the specific contributions of the MSSM Higgs bosons to δS and δT. As indicated above, the sum of these contributions is finite after subtracting out the contribution of the Standard Model Higgs boson with $m_{\phi^0} = m_{h^0}$. In contrast to the Standard Model where the Higgs contributions to S and T grow logarithmically with Higgs mass, the contributions of the MSSM Higgs bosons smoothly decouple as the Higgs masses become large. This behavior is easy to understand. According to the results of section 3, the mass of h^0 cannot be arbitrarily large—it is bounded at tree level by m_Z. All other Higgs masses can become large by taking $m_{A^0} \gg m_Z$. In this limit, we see that $m_{H^\pm} \simeq m_{H^0} \simeq m_{A^0}$ and $m_{h^0} \simeq m_Z|\cos 2\beta|$. However, in this limit, the large Higgs masses are due to the large value of the mass parameter m_{12} [see eq. (18)] rather than a large Higgs self-coupling (which is the case in the large Higgs mass limit of the Standard Model). In particular, the Higgs self-couplings in the MSSM are gauge couplings which can never become large. As a result, the decoupling theorem applies, and one must find that δS and δT approach zero quadratically as $m_{A^0} \to \infty$. This result can be generalized to all other sectors of the MSSM! All MSSM contributions to S, T and U vanish in the limit of large supersymmetry-breaking mass parameters [37,38]. In this limit, the effects of the supersymmetric particles (and all Higgs bosons beyond h^0) smoothly decouple; the resulting low-energy effective theory at the scale m_Z is precisely that of the Standard Model.

The results of an exact one-loop computation of the MSSM Higgs contributions to S and T are given in Appendix C [38]. (See refs. [25,39-41] for previous work on radiative corrections in two-Higgs doublet models.) Numerical results are shown in figs. 3 and 4. To understand why the numerical values for the MSSM-Higgs contributions to δS and δT are so small, it is instructive to evaluate the corresponding expressions of Appendix C in the limit of large m_{A^0}. I find*

$$\delta S(\text{MSSM}-\text{Higgs}) \simeq \frac{m_Z^2(\sin^2 2\beta - 2\cos^2\theta_W)}{24\pi m_{A^0}^2}, \quad (33)$$

$$\delta T(\text{MSSM}-\text{Higgs}) \simeq \frac{m_Z^2(\cos^2\theta_W - \sin^2 2\beta)}{48\pi m_{A^0}^2 \sin^2\theta_W}. \quad (34)$$

* Asymptotically, $\delta U(\text{MSSM–Higgs}) = \mathcal{O}(m_Z^4/m_A^4)$, which is completely negligible.

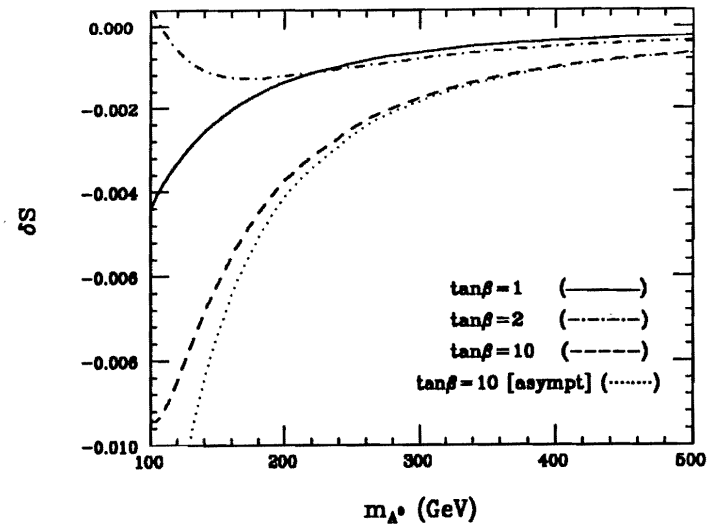

Fig. 3. The contribution to the S parameter from the MSSM Higgs sector relative to the Standard Model with Higgs mass set equal to m_{h^0}, as a function of m_{A^0}. Three curves corresponding to $\tan\beta = 1$, 2, and 10 are shown. For comparison, the dotted curve depicts the asymptotic prediction [eq. (33)] for $\tan\beta = 10$.

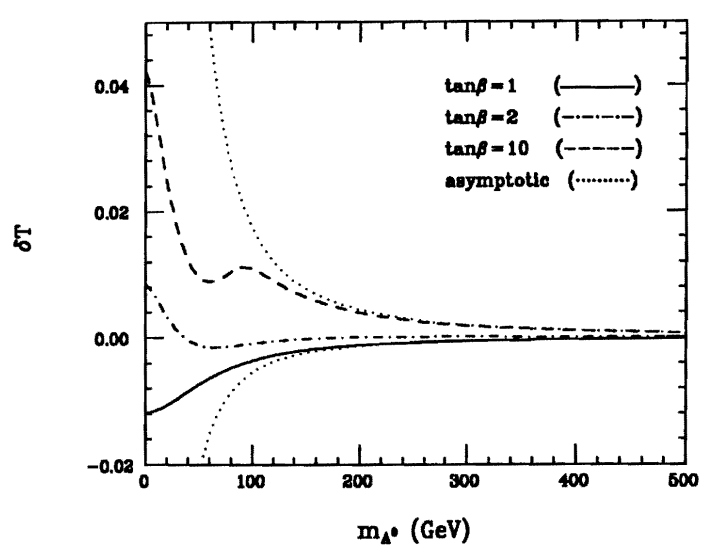

Fig. 4. The contribution to the T parameter from the MSSM Higgs sector relative to the Standard Model with Higgs mass set equal to m_{h^0}, as a function of m_{A^0}. Three curves corresponding to $\tan\beta = 1$, 2, and 10 are shown. For comparison, the two dotted curves depict the asymptotic predictions [eq. (34)] for $\tan\beta = 1$ and 10 respectively. The ρ parameter is related to T via $\delta\rho = \alpha\delta T$, where α is the fine structure constant.

A recent analysis of S, T and U based on LEP data (assuming a RSM where $m_t = m_{\phi^0} = m_Z$) reported in ref. 30 yields: $\delta S = -0.97 \pm 0.67$, $\delta T = -0.18 \pm 0.51$ and $\delta U = 0.07 \pm 0.97$. It is hard to imagine that the these quantities could ever be measured to an accuracy better than 0.1 One must also consider the possibility of other contributions to δS and δT. As long as m_t is not well known, there will be m_t dependence in these quantities (entering through the m_t choice of the RSM). Moreover, in the supersymmetric model, δS and δT would also acquire contributions from other MSSM sectors which, although small, are nearly always larger than the MSSM-Higgs contributions shown above [38]. Thus, I conclude that virtual effects of the MSSM Higgs sector will never be detected via its oblique radiative corrections.

One class of processes for which virtual Higgs effects could be important are those involving external b or t quarks. Here, I shall briefly focus on processes involving B-mesons. In such cases, vertex corrections and box diagrams that involve an intermediate t-quark and charged Higgs boson can be substantial, because $g_{H^-t\bar{b}}$ contains a piece proportional to $m_t \cot\beta/m_W$ [see eq. (16)]. Thus the impact of such contributions can be significant for small $\tan\beta$ and $m_{H^\pm}$. Three examples of relevant processes studied in the literature are: (i) charged Higgs box diagram contributions to B^0–$\overline{B^0}$ mixing [42-45, 16] (briefly mentioned at the end of section 2); (ii) the charged Higgs vertex correction to $Z \to b\bar{b}$ [46]; and (iii) the charged Higgs vertex corrections to various rare b-decays [47,43-45] such as $b \to s\gamma$, $b \to s\ell^+\ell^-$, $b \to sg$ and $b \to s\nu\bar{\nu}$. Of course, if the two-Higgs-doublet model is a piece of the MSSM, then there will also be one-loop supersymmetric particle contributions to all of the processes mentioned above. Some of these contributions (*e.g.*, loops containing top-squarks) could dominate over the virtual charged Higgs effects [44,46].

Among the rare b-decays, the charged Higgs contribution to $b \to s\gamma$ is perhaps the most promising. The theoretical prediction for this rate in the Standard Model is $BR(B \to K\gamma + X) \simeq 3.6 \times 10^{-4}$ (4.1×10^{-4}), for $m_t = 150$ (200) GeV, where leading log QCD corrections have been included. Incorporating the charged Higgs contribution [assuming an $H^-t\bar{b}$ coupling specified in eq. (16)] yields results for this branching ratio shown in fig. 5. These results correspond to an enhancement over the Standard Model expectation as shown in fig. 6. Whether effects of the charged Higgs boson can be detected in this way (or interesting limits set) depends on the reliability of the Standard Model prediction. At present, this prediction is reliable to within a factor of two [47]. Improved theoretical analysis as well as more B-decay data will be required before definite conclusions can be drawn.

In summary, the only potentially important virtual Higgs boson corrections to Standard Model processes arise either through oblique radiative corrections (*i.e.*, Higgs loop corrections to vector boson propagators), or through charged Higgs vertex and box diagram corrections to processes with external b and/or t quarks. I

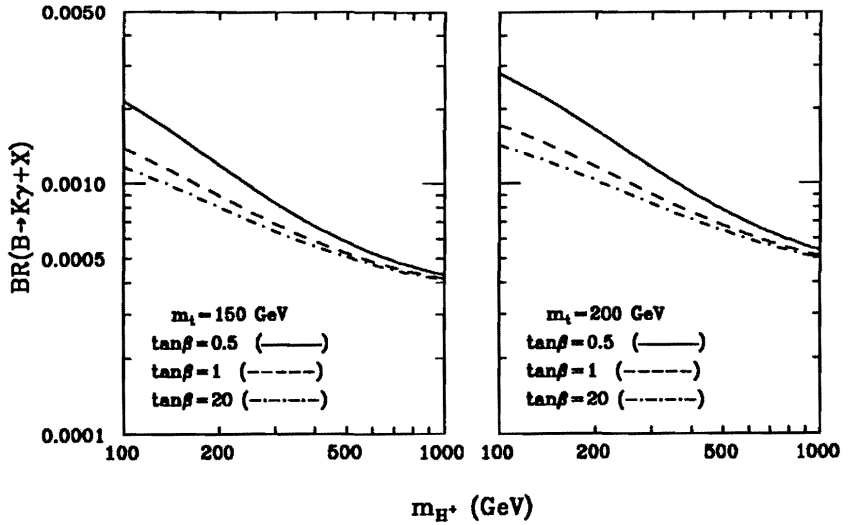

Fig. 5. The branching ratio for $B \to K\gamma + X$ in the two-Higgs-doublet model as a function of the charged Higgs mass for $m_t = 150$ and 200 GeV and various choices for $\tan\beta$, assuming an $H^- t\bar{b}$ coupling given by eq. (16). This graph is based on calculations of ref. 45.

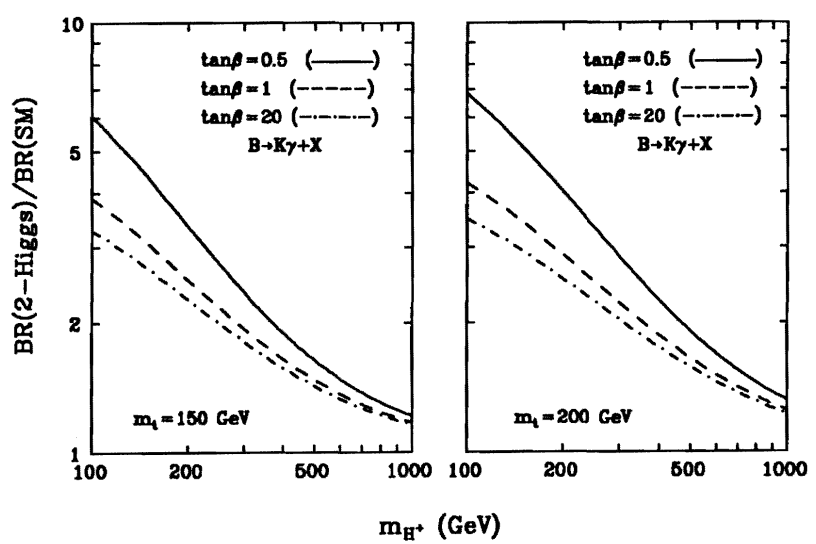

Fig. 6. The ratio of $BR(B \to K\gamma + X)$ in the two-Higgs-doublet model relative to its predicted value in the Standard Model (SM) as a function of the charged Higgs mass for $m_t = 150$ and 200 GeV and various choices for $\tan\beta$, assuming an $H^- t\bar{b}$ coupling given by eq. (16). This graph is based on calculations of ref. 45.

have shown above that in the MSSM, Higgs-mediated oblique radiative corrections are too small to be observed. This leaves heavy quark processes as the only possible arena for observable Higgs-mediated radiative corrections.

5. A Theoretical Upper Limit on the Lightest MSSM Higgs Mass

The tree-level Higgs mass predictions of section 3 have important phenomenological consequences. For example, the bound $m_{h^0} \leq m_Z$, if reliable, would have significant implications for future experiments at LEP-II. In principle, experiments running at LEP-II operating at $\sqrt{s} = 200$ GeV and design luminosity would either discover the Higgs boson (via $e^+e^- \to h^0 Z$) or rule out the MSSM. (Whether this is possible to do in practice depends on whether Higgs bosons with $m_{h^0} \approx m_Z$ can be detected [48].) However, $m_{h^0} \leq m_Z$ need not be respected when radiative corrections are incorporated. In the radiative corrections to the neutral CP-even Higgs squared-mass matrix, the 22-element is shifted by a term proportional to $(g^2 m_t^4/m_W^2)\ln(M_{\tilde{t}}^2/m_t^2)$ [49-51]. Such a term arises from an incomplete cancellation between top-quark and top-squark loop contributions to the neutral Higgs boson self-energy. If m_t is large, this term significantly alters the tree-level predictions.

Hempfling and I computed the exact one-loop expression for the light Higgs mass bound, as a function of all the relevant supersymmetric parameters [49]. This bound is saturated in the formal limit where $\tan\beta \to \infty$ (with all down-type fermions masses set equal to zero) and $m_{A^0} \geq m_Z$, m_{h^0}. The expression we obtained is quite cumbersome, although straightforward to evaluate numerically. However, it is useful to display an approximate expression, valid for a certain range of supersymmetric parameters. If all supersymmetric mass parameters are roughly of order $M_{\rm SUSY}$ and if $m_Z < m_t \ll M_{\rm SUSY}$, then

$$
\begin{aligned}
m_{h^0}^2 - m_Z^2 \lesssim \frac{3g^2 m_Z^2}{16\pi^2 c_W^2}\Bigg\{ & \ln\left(\frac{M_{\tilde{Q}}^2}{m_t^2}\right)\left[\frac{2m_t^4 - m_t^2 m_Z^2}{m_Z^4} + \tfrac{1}{6}\left(1 - \tfrac{8}{3}s_W^2 + \tfrac{32}{9}s_W^4\right)\right] \\
& + \ln\left(\frac{M_{\tilde{Q}}^2}{m_Z^2}\right)\left[\tfrac{1}{3}\left(1 - \tfrac{8}{3}s_W^2 + \tfrac{32}{9}s_W^4\right) + \tfrac{1}{2}\left(1 - \tfrac{4}{3}s_W^2 + \tfrac{8}{9}s_W^4\right)\right. \\
& \left. + \tfrac{1}{3}\left(1 - 2s_W^2 + 4s_W^4\right)\right] + \frac{m_t^2}{3m_Z^2}\Bigg\} \\
& - \frac{g^2 m_Z^2}{48\pi^2 c_W^2}\left[(27 - 54s_W^2 + 32s_W^4)\ln\left(\frac{M_{\tilde{X}}^2}{m_Z^2}\right) - (1 - 2s_W^2 + 2s_W^4)\ln\left(\frac{m_{A^0}^2}{m_Z^2}\right)\right],
\end{aligned}
\tag{35}
$$

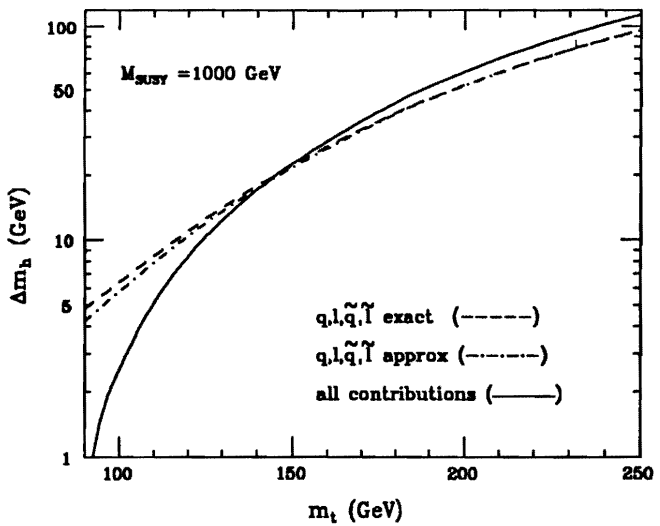

Fig. 7. The light Higgs mass bound ($m_{h^0} \leq m_Z + \Delta m_h$) including one-loop radiative corrections. The dashed line denotes the contribution to Δm_h due to three generations of quarks, leptons, and their supersymmetric scalar partners (assumed to have a common soft-supersymmetry breaking mass of $M_{\tilde{Q}} = 1$ TeV); $\tilde{t}_L$–$\tilde{t}_R$ mixing is neglected. The dot-dashed line is a plot of the corresponding contribution to eq. (35). The solid line includes *all* contributions to the exact one-loop calculation of Δm_h where all supersymmetric mass parameters (including the A parameter that controls top-squark mixing) are equal to $M_{\rm SUSY} = 1$ TeV. Taken from ref. [49].

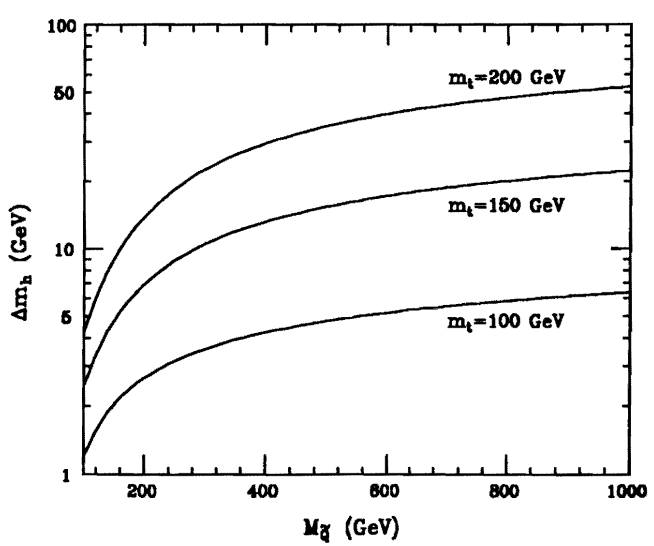

Fig. 8. The contribution to Δm_h of three generations of quarks, leptons, and their supersymmetric scalar partners as a function of the common soft-supersymmetry breaking scalar mass, $M_{\tilde{Q}}$, for three different values of the top quark mass. Squark mixing is neglected.

where $s_W \equiv \sin\theta_W$, $c_W \equiv \cos\theta_W$, $M_{\tilde{Q}}$ is a common soft-supersymmetry-breaking diagonal squark mass term, and $M_{\tilde{\chi}}$ is a common neutralino/chargino mass. The radiatively corrected light Higgs mass bound will be written as

$$m_{h^0} \leq m_Z + \Delta m_h\,, \tag{36}$$

which defines the quantity Δm_h. A numerical calculation of Δm_h is displayed in fig. 7. As advertised, the dominant correction to the tree-level formula increases as the fourth power of m_t, and therefore can be quite large. Nevertheless, for values of $m_t \lesssim 250$ GeV, the perturbative one-loop calculation is reliable. This can be verified by estimating the largest two-loop contributions to Δm_h and showing that the one-loop result is stable [52].

It is also evident from eq. (35) that the dependence of the squared Higgs mass shift on $M^2_{\tilde{Q}}$ is logarithmic. Thus, even if $M_{\tilde{Q}}$ is significantly smaller than 1 TeV, Δm_h can be appreciable if m_t is sufficiently large. This is illustrated in fig. 8, where Δm_h is plotted as a function of $M_{\tilde{Q}}$ for $m_t = 100$, 150 and 200 GeV. These results are based on an exact numerical one-loop computation; the approximate formula given in eq. (35) is unreliable for values of $M_{\tilde{Q}}$ approaching m_t.

6. Radiative Corrections to the MSSM Higgs Masses

One can also compute radiative corrections to the full CP-even Higgs mass-squared matrix [51,53–58]. Full one-loop computations can be found in refs. 53 and 57. Here, I will present the results based on a calculation of the mass-squared matrix in which all leading logarithmic terms are included (see ref. 54 for details). We take the supersymmetry breaking scale ($M_{\rm SUSY}$) to be somewhat larger than the electroweak scale. For simplicity, we assume that the masses of all supersymmetric particles (squarks, sleptons, neutralinos and charginos) are roughly degenerate and of order $M_{\rm SUSY}$. This means that various soft-supersymmetry breaking parameters such as the diagonal squark mass parameter, $M_{\tilde{Q}}$, and the gaugino Majorana mass terms, as well as the supersymmetric Higgs mass parameter are all roughly equal to $M_{\rm SUSY}$. Admittedly, this is a crude approximation. However, deviations from this assumption will lead to non-leading logarithmic corrections which tend to be small if the supersymmetric particles are not widely split in mass. Moreover, the procedure outlined below can be modified to incorporate the largest non-leading logarithmic contributions that arise in the case of multiple supersymmetric particle thresholds and/or large squark mixing.

The leading logarithmic expressions for Higgs masses are obtained from eqs. (4) and (5) by treating the λ_i as running parameters evaluated at the electroweak scale,

$M_{\rm weak}$. In addition, we identify the W and Z masses by

$$\begin{aligned} m_W^2 &= \tfrac{1}{4}g^2(v_1^2+v_2^2)\,, \\ m_Z^2 &= \tfrac{1}{4}(g^2+g'^2)(v_1^2+v_2^2)\,, \end{aligned} \tag{37}$$

where the running gauge couplings are also evaluated at $M_{\rm weak}$. Of course, the gauge couplings, g and g' are known from experimental measurements which are performed at the scale $M_{\rm weak}$. The $\lambda_i(M_{\rm weak}^2)$ are determined from supersymmetry. Namely, if supersymmetry were unbroken, then the λ_i would be fixed according to eq. (17). Since supersymmetry is broken, we regard eq. (17) as boundary conditions for the running parameters, valid at (and above) the energy scale $M_{\rm SUSY}$. That is, we take

$$\begin{aligned} \lambda_1(M_{\rm SUSY}^2) &= \lambda_2(M_{\rm SUSY}^2) = \tfrac{1}{4}[g^2(M_{\rm SUSY}^2)+g'^2(M_{\rm SUSY}^2)], \\ \lambda_3(M_{\rm SUSY}^2) &= \tfrac{1}{4}\left[g^2(M_{\rm SUSY}^2)-g'^2(M_{\rm SUSY}^2)\right], \\ \lambda_4(M_{\rm SUSY}^2) &= -\tfrac{1}{2}g^2(M_{\rm SUSY}^2), \\ \lambda_5(M_{\rm SUSY}^2) &= \lambda_6(M_{\rm SUSY}^2) = \lambda_7(M_{\rm SUSY}^2) = 0\,, \end{aligned} \tag{38}$$

in accordance with the tree-level relations of the MSSM. At scales below $M_{\rm SUSY}$, the gauge and quartic couplings evolve according to the renormalization group equations (RGEs) of the non-supersymmetric two-Higgs-doublet model given in eqs. (B.5)–(B.7). These equations are of the form:

$$\frac{dp_i}{dt} = \beta_i(p_1,p_2,\ldots) \qquad \text{with } t \equiv \ln\mu^2\,, \tag{39}$$

where μ is the energy scale, and the p_i are the parameters of the theory ($p_i = g_j^2, \lambda_k, \ldots$). The relevant β-functions can be found in Appendix B. The boundary conditions together with the RGEs imply that, at the leading-log level, λ_5, λ_6 and λ_7 are zero at all energy scales. Solving the RGEs with the supersymmetric boundary conditions at $M_{\rm SUSY}$, one can determine the λ_i at the weak scale. The resulting values for $\lambda_i(M_{\rm weak})$ are then inserted into eqs. (4) and (5) to obtain the radiatively corrected Higgs masses. Having solved the one-loop RGEs, the Higgs masses thus obtained include the leading logarithmic radiative corrections summed to all orders in perturbation theory.

The RGEs can be solved by numerical analysis on the computer. But it is instructive to solve the RGEs iteratively. In first approximation, we can take the right hand side of eq. (39) to be independent of μ^2. That is, we compute the β_i by evaluating the parameters p_i at the scale $\mu = M_{\rm SUSY}$. Then, integration of the

RGEs is trivial, and we obtain

$$p_i(M_{\rm weak}^2) = p_i(M_{\rm SUSY}^2) - \beta_i \ln\left(\frac{M_{\rm SUSY}^2}{M_{\rm weak}^2}\right)\,. \tag{40}$$

Note that this iterative solution corresponds to computing the one-loop radiative corrections in which only terms proportional to $\ln M_{\rm SUSY}^2$ are kept. It is straightforward to work out the one-loop leading logarithmic expressions for the λ_i and the Higgs masses. First consider the charged Higgs mass. Since $\lambda_5(\mu^2) = 0$ at all scales, we need only consider λ_4. Evaluating β_{λ_4} at $\mu = M_{\rm SUSY}$, we compute

$$\begin{aligned} \lambda_4(m_W^2) = -\tfrac{1}{2}g^2 - \frac{1}{32\pi^2}\Bigg[&\left(\tfrac{4}{3}N_g + \tfrac{1}{6}N_H - \tfrac{10}{3}\right)g^4 + 5g^2g'^2 \\ &- \frac{3g^4}{2m_W^2}\left(\frac{m_t^2}{s_\beta^2}+\frac{m_b^2}{c_\beta^2}\right) + \frac{3g^2m_t^2m_b^2}{s_\beta^2c_\beta^2m_W^4}\Bigg]\ln\frac{M_{\rm SUSY}^2}{m_W^2}\,. \end{aligned} \tag{41}$$

The terms proportional to the number of generations $N_g = 3$ and the number of Higgs doublets $N_H = 2$ that remain in the low-energy effective theory at the scale $\mu = m_W$ have their origin in the running of g^2 from $M_{\rm SUSY}$ down to m_W. In deriving this expression, I have taken $M_{\rm weak} = m_W$. This is a somewhat arbitrary decision, since another reasonable choice would yield a result that differs from eq. (41) by a non-leading logarithmic term. Comparisons with a more complete calculation show that one should choose $M_{\rm weak} = m_W$ in computations involving the charged Higgs (and gauge) sector, and $M_{\rm weak} = m_Z$ in computations involving the neutral sector.

The above analysis also assumes that $m_t \sim \mathcal{O}(m_W)$. Although this is a good assumption, we can improve the above result somewhat when $m_t > m_W$ by decoupling the (t,b) weak doublet from the low-energy theory for scales below m_t. The terms in eq. (41) that are proportional to m_t^2 and/or m_b^2 arise from self-energy diagrams containing a tb loop. Thus, such a term should not be present for $m_W \le \mu \le m_t$. In addition, we recognize the term in eq. (41) proportional to the number of generations N_g as arising from the contributions to the self-energy diagrams containing either quark or lepton loops (and their supersymmetric partners). To identify the contribution of the tb loop to this term, simply write

$$N_g = \tfrac{1}{4}N_g(N_c+1) = \tfrac{1}{4}N_c + \tfrac{1}{4}[N_c(N_g-1)+N_g]\,, \tag{42}$$

where $N_c = 3$ colors. Thus, we identify $\frac{1}{4}N_c$ as the piece of the term proportional to N_g that is due to the tb loop. The rest of this term is then attributed to the

lighter quarks and leptons. Finally, the remaining terms in eq. (41) are due to the contributions from the gauge and Higgs boson sector. The final result is [59]

$$\lambda_4(m_W^2) = -\tfrac{1}{2}g^2 - \frac{N_c g^4}{32\pi^2}\left[\frac{1}{3} - \frac{1}{2m_W^2}\left(\frac{m_t^2}{s_\beta^2} + \frac{m_b^2}{c_\beta^2}\right) + \frac{m_t^2 m_b^2}{s_\beta^2 c_\beta^2 m_W^4}\right]\ln\frac{M_{\rm SUSY}^2}{m_t^2}$$
$$- \frac{1}{96\pi^2}\left\{\left[N_c(N_g-1) + N_g + \tfrac{1}{2}N_H - 10\right]g^4 + 15g^2g'^2\right\}\ln\frac{M_{\rm SUSY}^2}{m_W^2}. \tag{43}$$

Inserting this result (and $\lambda_5 = 0$) into eq. (4), we obtain the one-loop leading-log formula for the charged Higgs mass

$$m_{H^\pm}^2 = m_A^2 + m_W^2 + \frac{N_c g^2}{32\pi^2 m_W^2}\left[\frac{2m_t^2 m_b^2}{s_\beta^2 c_\beta^2} - m_W^2\left(\frac{m_t^2}{s_\beta^2} + \frac{m_b^2}{c_\beta^2}\right) + \tfrac{2}{3}m_W^4\right]\ln\frac{M_{\rm SUSY}^2}{m_t^2}$$
$$+ \frac{m_W^2}{48\pi^2}\left\{\left[N_c(N_g-1) + N_g + \tfrac{1}{2}N_H - 10\right]g^2 + 15g'^2\right\}\ln\frac{M_{\rm SUSY}^2}{m_W^2}. \tag{44}$$

Since this derivation makes use of the two-Higgs-doublet RGEs for the λ_i, there is an implicit assumption that the full two-doublet Higgs spectrum survives in the low-energy effective theory at $\mu = m_W$. This means that we *must* take $N_H = 2$ in the formulae above. It also means that m_{A^0} cannot be much larger than m_W.* Of course, eq. (44) is only a one-loop result. This result is improved by using the full RGE solution to $\lambda_4(m_W^2)$

$$m_{H^\pm}^2 = m_{A^0}^2 - \tfrac{1}{2}\lambda_4(m_W^2)(v_1^2 + v_2^2). \tag{45}$$

Although the leading-log formula for $m_{H^\pm}$ [eq. (44)] gives a useful indication as to the size of the radiative corrections, non-leading logarithmic contributions can also be important in certain regions of parameter space. A more complete set of radiative corrections can be found in the literature [53,59-62]. In the numerical results to be exhibited below, important non-leading corrections to the charged Higgs mass are also included (as described in ref. 59). However, it should be emphasized that the radiative corrections to the charged Higgs mass are significant only for $\tan\beta < 1$, a region of MSSM parameter space not favored in supersymmetric models.

* If $m_{A^0} \sim \mathcal{O}(M_{\rm SUSY})$, then $H^\pm$, H^0 and A^0 would all have masses of order $M_{\rm SUSY}$, and the effective low-energy theory below $M_{\rm SUSY}$ would be that of the minimal Standard Model. Clearly, the above computation would not be appropriate in this case.

The computation of the neutral CP-even Higgs masses follows a similar procedure. The results are summarized below [54]. From eq. (5), we see that we only need results for λ_1, λ_2 and $\widetilde{\lambda}_3 \equiv \lambda_3 + \lambda_4 + \lambda_5$. (Recall that $\lambda_5 = \lambda_6 = \lambda_7 = 0$ at all energy scales.) By iterating the corresponding RGEs as before, we end up with

$$\lambda_1(m_Z^2) = \tfrac{1}{4}[g^2 + g'^2](m_Z^2) + \frac{g^4}{384\pi^2 c_W^4}\left[P_t \ln\left(\frac{M_{\rm SUSY}^2}{m_t^2}\right)\right.$$
$$\left. + \left(12N_c\frac{m_b^4}{m_Z^4 c_\beta^4} - 6N_c\frac{m_b^2}{m_Z^2 c_\beta^2} + P_f + P_g + P_{2H}\right)\ln\left(\frac{M_{\rm SUSY}^2}{m_Z^2}\right)\right],$$
$$\lambda_2(m_Z^2) = \tfrac{1}{4}[g^2 + g'^2](m_Z^2) + \frac{g^4}{384\pi^2 c_W^4}\left[\left(P_f + P_g + P_{2H}\right)\ln\left(\frac{M_{\rm SUSY}^2}{m_Z^2}\right)\right.$$
$$\left. + \left(12N_c\frac{m_t^4}{m_Z^4 s_\beta^4} - 6N_c\frac{m_t^2}{m_Z^2 s_\beta^2} + P_t\right)\ln\left(\frac{M_{\rm SUSY}^2}{m_t^2}\right)\right],$$
$$\widetilde{\lambda}_3(m_Z^2) = -\tfrac{1}{4}[g^2 + g'^2](m_Z^2) - \frac{g^4}{384\pi^2 c_W^4}\left[\left(-3N_c\frac{m_t^2}{m_Z^2 s_\beta^2} + P_t\right)\ln\left(\frac{M_{\rm SUSY}^2}{m_t^2}\right)\right.$$
$$\left. + \left(-3N_c\frac{m_b^2}{m_Z^2 c_\beta^2} + P_f + P_g' + P_{2H}'\right)\ln\left(\frac{M_{\rm SUSY}^2}{m_Z^2}\right)\right], \tag{46}$$

where

$$\begin{aligned}
P_t &\equiv N_c(1 - 4e_u s_W^2 + 8e_u^2 s_W^4),\\
P_f &\equiv N_g\{N_c[2 - 4s_W^2 + 8(e_d^2 + e_u^2)s_W^4] + [2 - 4s_W^2 + 8s_W^4]\} - P_t,\\
P_g &\equiv -44 + 106s_W^2 - 62s_W^4,\\
P_g' &\equiv 10 + 34s_W^2 - 26s_W^4,\\
P_{2H} &\equiv -10 + 2s_W^2 - 2s_W^4,\\
P_{2H}' &\equiv 8 - 22s_W^2 + 10s_W^4.
\end{aligned} \tag{47}$$

In the above formulae, the electric charges of the quarks are $e_u = 2/3$, $e_d = -1/3$, and the subscripts t, f, g and $2H$ indicate that these are the contributions from the top quark, the fermions (leptons and quarks excluding the top quark), the gauge bosons and the two Higgs doublets (and corresponding supersymmetric partners), respectively. As in the derivation of $\lambda_4(m_W^2)$ above, we have improved our analysis by removing the effects of top-quark loops below $\mu = m_t$. This requires a careful treatment of the evolution of g and g' at scales below $\mu = m_t$. The correct procedure is somewhat subtle, since the full electroweak gauge symmetry is broken

below top-quark threshold; for further details, see ref. 54. However, the following pedestrian technique works: consider the RGE for $g^2 + g'^2$ valid for $\mu < M_{\rm SUSY}$

$$\frac{d}{dt}(g^2+g'^2) = \frac{1}{96\pi^2}\left[\left(8g^4+\tfrac{40}{3}g'^4\right)N_g + (g^4+g'^4)N_H - 44g^4\right]. \tag{48}$$

This equation is used to run $g^2+g'^2$, which appears in eq. (38), from $M_{\rm SUSY}$ down to m_Z. As before, we identify the term proportional to N_g as corresponding to the fermion loops. We can explicitly extract the t-quark contribution by noting that

$$\begin{aligned} N_g\left(8g^4+\tfrac{40}{3}g'^4\right) &= \frac{g^4 N_g}{c_W^4}\left[\tfrac{64}{3}s_W^4 - 16s_W^2 + 8\right] \\ &= \frac{g^4}{c_W^4}\Big\{N_c[1+(N_g-1)](1-4e_u s_W^2+8e_u^2 s_W^4) \\ &\quad + N_c N_g(1+4e_d s_W^2+8e_d^2 s_W^4) + N_g(2-4s_W^2+8s_W^4)\Big\}, \end{aligned} \tag{49}$$

where in the first line of the last expression, the term proportional to 1 corresponds to the t-quark contribution while the term proportional to $N_g - 1$ accounts for the u and c-quarks; the second line contains the contributions from the down-type quarks and leptons respectively. Thus, iterating to one-loop,

$$\begin{aligned} [g^2+g'^2](M_{\rm SUSY}^2) &= [g^2+g'^2](m_Z^2) + \frac{g^4}{96\pi^2 c_W^4}\Bigg[P_t \ln\left(\frac{M_{\rm SUSY}^2}{m_t^2}\right) \\ &\quad + \left[P_f + (s_W^4+c_W^4)N_H - 44c_W^4\right]\ln\left(\frac{M_{\rm SUSY}^2}{m_Z^2}\right)\Bigg]. \end{aligned} \tag{50}$$

This result and terms that are proportional to m_t^2 and m_t^4 yield the terms in eq. (46) that contain $\ln(M_{\rm SUSY}^2/m_t^2)$.

The final step is to insert the expressions obtained in eq. (46) into eq. (5). The resulting matrix elements for the mass-squared matrix to one-loop leading logarithmic accuracy are given by

$$\begin{aligned} \mathcal{M}_{11}^2 &= m_{A^0}^2 s_\beta^2 + m_Z^2 c_\beta^2 + \frac{g^2 m_Z^2 c_\beta^2}{96\pi^2 c_W^2}\Bigg[P_t \ln\left(\frac{M_{\rm SUSY}^2}{m_t^2}\right) \\ &\quad + \left(12N_c\frac{m_b^4}{m_Z^4 c_\beta^4} - 6N_c\frac{m_b^2}{m_Z^2 c_\beta^2} + P_f + P_g + P_{2H}\right)\ln\left(\frac{M_{\rm SUSY}^2}{m_Z^2}\right)\Bigg] \\ \mathcal{M}_{22}^2 &= m_{A^0}^2 c_\beta^2 + m_Z^2 s_\beta^2 + \frac{g^2 m_Z^2 s_\beta^2}{96\pi^2 c_W^2}\Bigg[\left(P_f + P_g + P_{2H}\right)\ln\left(\frac{M_{\rm SUSY}^2}{m_Z^2}\right) \\ &\quad + \left(12N_c\frac{m_t^4}{m_Z^4 s_\beta^4} - 6N_c\frac{m_t^2}{m_Z^2 s_\beta^2} + P_t\right)\ln\left(\frac{M_{\rm SUSY}^2}{m_t^2}\right)\Bigg] \\ \mathcal{M}_{12}^2 &= -s_\beta c_\beta\Bigg\{m_{A^0}^2 + m_Z^2 + \frac{g^2 m_Z^2}{96\pi^2 c_W^2}\Bigg[\left(P_t - 3N_c\frac{m_t^2}{m_Z^2 s_\beta^2}\right)\ln\left(\frac{M_{\rm SUSY}^2}{m_t^2}\right) \\ &\quad + \left(-3N_c\frac{m_b^2}{m_Z^2 c_\beta^2} + P_f + P_g' + P_{2H}'\right)\ln\left(\frac{M_{\rm SUSY}^2}{m_Z^2}\right)\Bigg]\Bigg\}, \end{aligned} \tag{51}$$

Diagonalizing this matrix [eq. (51)] yields the radiatively corrected CP-even Higgs masses and mixing angle α. One can check that if $m_b = 0$ and $\sin\beta = 1$, then $m_{h^0}^2 = \mathcal{M}_{22}^2$ reproduces the leading logarithmic terms of eq. (35) (after putting $M_{\tilde{Q}} = M_{\tilde{\chi}} = M_{\rm SUSY}$ and $m_{A^0} = m_Z$).

The analysis presented above assumes that m_{A^0} is not much larger than $\mathcal{O}(m_Z)$ so that the Higgs sector of the low-energy effective theory contains the full two-Higgs-doublet spectrum. On the other hand, if $m_{A^0} \gg m_Z$, then only h^0 remains in the low-energy theory. In this case, we must integrate out the heavy Higgs doublet, in which case one of the mass eigenvalues of $\mathcal{M}_{ij}^2$ [eq. (19)] is much larger than the weak scale. Then, in order to obtain the effective Lagrangian at $M_{\rm weak}$, we first have to run the various coupling constants to the threshold m_{A^0}. Then we diagonalize the Higgs mass matrix and express the Lagrangian in terms of the mass eigenstates. Notice that in this case the mass eigenstate h^0 is directly related to the field with the non-zero VEV [*i.e.*, $\beta(m_{A^0}) = \alpha(m_{A^0}) + \pi/2 + \mathcal{O}(m_Z^2/m_{A^0}^2)$]. Below m_{A^0} there remains only the Standard Model Higgs doublet $\phi \equiv c_\beta\Phi_1 + s_\beta\Phi_2$. The potential is

$$\mathcal{V} = m_\phi^2(\phi^\dagger\phi) + \tfrac{1}{2}\lambda(\phi^\dagger\phi)^2, \tag{52}$$

and the light CP-even Higgs mass is obtained using $m_{h^0}^2 = \lambda v^2$. The RGE in the

Standard Model for λ is [63,64]

$$16\pi^2\beta_\lambda = 6\lambda^2 + \tfrac{3}{8}\left[2g^4 + (g^2+g'^2)^2\right] - 2\sum_i N_{c_i} h_{f_i}^4 - \lambda\left(\tfrac{9}{2}g^2 + \tfrac{3}{2}g'^2 - 2\sum_i N_{c_i} h_{f_i}^2\right), \tag{53}$$

where the summation is over all fermions with $h_{f_i} = gm_{f_i}/(\sqrt{2}m_W)$. The RGEs for the gauge couplings are obtained from β_{g^2} and $\beta_{g'^2}$ given in Appendix B by putting $N_H = 1$. In addition, we require the boundary condition for λ at m_{A^0}

$$\begin{aligned}\lambda(m_{A^0}) &= \left[c_\beta^4\lambda_1 + s_\beta^4\lambda_2 + 2s_\beta^2c_\beta^2(\lambda_3+\lambda_4+\lambda_5) + 4c_\beta^3 s_\beta\lambda_6 + 4c_\beta s_\beta^3\lambda_7\right](m_{A^0}) \\ &= \left[\tfrac{1}{4}(g^2+g'^2)c_{2\beta}^2\right](m_{A^0}) + \frac{g^4}{384\pi^2c_W^4}\ln\left(\frac{M_{\rm SUSY}^2}{m_{A^0}^2}\right) \\ &\quad\times\left[12N_c\left(\frac{m_t^4}{m_Z^4}+\frac{m_b^4}{m_Z^4}\right) + 6N_c c_{2\beta}\left(\frac{m_t^2}{m_Z^2}-\frac{m_b^2}{m_Z^2}\right)\right. \\ &\quad\left. + c_{2\beta}^2(P_t+P_f) + (s_\beta^4+c_\beta^4)(P_g+P_{2H}) - 2s_\beta^2c_\beta^2(P_g'+P_{2H}')\right],\end{aligned} \tag{54}$$

where $(g^2+g'^2)c_{2\beta}^2$ is to be evaluated at the scale m_{A^0} as indicated. The RGE for $g^2+g'^2$ was given in eq. (48); note that at scales below m_A we must set $N_H = 1$. Finally, we must deal with implicit scale dependence of $c_{2\beta}^2$. Since the fields Φ_i $(i=1,2)$ change with the scale, it follows that $\tan\beta$ scales like the ratio of the two Higgs doublet fields, *i.e.*,

$$\frac{1}{\tan^2\beta}\frac{d\tan^2\beta}{dt} = \frac{\Phi_1^2}{\Phi_2^2}\frac{d}{dt}\left(\frac{\Phi_2^2}{\Phi_1^2}\right) = \gamma_2 - \gamma_1\,. \tag{55}$$

Thus we arrive at the RGE for $\cos 2\beta$ in terms of the anomalous dimensions γ_i given in eq. (B.6). Solving this equation iteratively to first order yields

$$c_{2\beta}^2(m_{A^0}) = c_{2\beta}^2(m_Z) + 4c_{2\beta}c_\beta^2 s_\beta^2(\gamma_1-\gamma_2)\ln\left(\frac{m_{A^0}^2}{m_Z^2}\right). \tag{56}$$

The one loop leading log expression for $m_{h^0}^2 = \lambda(m_Z)v^2$ can now be obtained by solving the RGEs above for $\lambda(m_Z)$ iteratively to first order using the boundary

condition given in eq. (54). The result is

$$\begin{aligned}m_{h^0}^2 &= m_Z^2c_{2\beta}^2(m_Z) + \frac{g^2m_Z^2}{96\pi^2c_W^2}\left\{\left[12N_c\frac{m_b^4}{m_Z^4} - 6N_cc_{2\beta}\frac{m_b^2}{m_Z^2} + c_{2\beta}^2P_f\right.\right. \\ &\quad\left. + (P_g+P_{2H})(s_\beta^4+c_\beta^4) - 2s_\beta^2c_\beta^2(P_g'+P_{2H}')\right]\ln\left(\frac{M_{\rm SUSY}^2}{m_Z^2}\right) \\ &\quad + \left[12N_c\frac{m_t^4}{m_Z^4} + 6N_cc_{2\beta}\frac{m_t^2}{m_Z^2} + c_{2\beta}^2P_t\right]\ln\left(\frac{M_{\rm SUSY}^2}{m_t^2}\right) \\ &\quad\left. - \left[(c_\beta^4+s_\beta^4)P_{2H} - 2c_\beta^2s_\beta^2P_{2H}' - P_{1H}\right]\ln\left(\frac{m_{A^0}^2}{m_Z^2}\right)\right\} + \mathcal{O}\left(\frac{m_Z^4}{m_{A^0}^2}\right),\end{aligned} \tag{57}$$

where the term proportional to

$$P_{1H} \equiv -9c_{2\beta}^4 + (1-2s_W^2+2s_W^4)c_{2\beta}^2\,, \tag{58}$$

corresponds to the Higgs boson contribution in the one-Higgs-doublet model. As a check, one can verify that eq. (35) is reproduced in the limit of large $\tan\beta$ (and $m_b = 0$).

The leading-log formulae presented above are expected to be accurate as long as: (i) there is one scale characterizing supersymmetric masses, $M_{\rm SUSY}$, which is large and sufficiently separated from m_Z (say, $M_{\rm SUSY} \gtrsim 500$ GeV), (ii) m_t is somewhat above m_Z (say, $m_t \gtrsim 125$ GeV) while still being small compared to $M_{\rm SUSY}$, and (iii) the squark mixing parameters are not unduly large. In particular, (ii) is an important condition—it is the dominance of the leading $m_t^4\ln(M_{\rm SUSY}^2/m_t^2)$ term that guarantees that the non-leading logarithmic terms are unimportant.* Under these conditions, the largest non-leading logarithmic term is of $\mathcal{O}(g^2m_t^2)$, which can be identified from a full one-loop computation as being the subdominant term relative to the leading $\mathcal{O}(g^2m_t^4\ln M_{\rm SUSY}^2)$ term in $\mathcal{M}_{22}^2$. Thus, we can make a minor improvement on our computation of the leading-log CP-even Higgs squared mass matrix by taking

$$\mathcal{M}^2 = \mathcal{M}_{\rm LL}^2 + \frac{N_cg^2m_t^2}{48\pi^2s_\beta^2c_W^2}\begin{pmatrix}0 & 0\\ 0 & 1\end{pmatrix} \tag{59}$$

where $\mathcal{M}_{\rm LL}^2$ is the leading-log CP-even Higgs squared mass matrix [given to one-loop in eq. (51)]. For $\beta = \pi/2$, this correction yields the non-leading-logarithmic

* In contrast, there is no leading logarithmic contribution to $m_{H^\pm}^2$ that grows with m_t^4. As a result, the non-leading logarithmic terms tend to be more important as discussed earlier.

term displayed in eq. (35). The shift of the light Higgs mass due to this non-leading-log correction is of order 1 GeV.

In the case of multiple and widely separated supersymmetric particle thresholds and/or large squark mixing (which is most likely in the top squark sector), new non-leading logarithmic contributions to the scalar mass-squared matrix can become important. In ref. 54, Hempfling and I show that such effects can be taken into account by modifying the boundary conditions of the λ_i at the supersymmetry breaking scale [eq. (38)], and by modifying the RGEs to account for multiple thresholds. In particular, we find that λ_5, λ_6 and λ_7 are no longer zero. If the new RGEs are solved iteratively to one loop, then the effects of the new boundary conditions are simply additive. As an example, suppose I allow for $\tilde{q}_L$–$\tilde{q}_R$ mixing in the third generation of squarks. The off-diagonal squark mass squared matrix element is given by [65]

$$M^2_{LR} = \begin{cases} m_b(A_b - \mu\tan\beta)\,, & \text{for } \tilde{b}_L\text{–}\tilde{b}_R \text{ mixing,} \\ m_t(A_t - \mu\cot\beta)\,, & \text{for } \tilde{t}_L\text{–}\tilde{t}_R \text{ mixing,} \end{cases} \tag{60}$$

where A_b and A_t are soft-supersymmetry breaking parameters and μ is the supersymmetric Higgs mass parameter [7]. Then, if we denote the one-loop leading log squared mass shifts obtained from eq. (51) by $(\Delta m^2)_{1\mathrm{LL}}$ then we obtain the following expressions for the neutral Higgs masses in the limit of large $\tan\beta$:

$$\begin{aligned}(m^2_{h^0} - m^2_Z)_{\beta=\pi/2} = (\Delta m^2_{h^0})_{1\mathrm{LL}} &- \frac{N_c g^2 m^2_W}{96\pi^2 M^4_{\tilde{Q}}}\left[\left(\frac{A_t m_t}{s_\beta m_W}\right)^4 + \left(\frac{\mu m_b}{c_\beta m_W}\right)^4\right] \\ &+ \frac{N_c g^2 m^2_W}{96\pi^2 M^2_{\tilde{Q}}}\left[\frac{12A^2_t m^4_t}{s^4_\beta m^4_W} - \frac{4A^2_t m^2_t}{s^2_\beta m^2_W c^2_W} + \frac{2\mu^2 m^2_b}{c^2_\beta m^2_W c^2_W}\right],\end{aligned} \tag{61}$$

and

$$(m^2_{H^0} - m^2_{A^0})_{\beta=\pi/2} = -\frac{N_c g^2 \mu^2}{96\pi^2 M^4_{\tilde{Q}}}\left(\frac{A^2_t m^4_t}{s^4_\beta m^2_W} + \frac{A^2_b m^4_b}{c^4_\beta m^2_W}\right), \tag{62}$$

assuming that $m_{A^0} > m_Z$ [if $m_{A^0} < m_Z$ then interchange m_{h^0} and m_{H^0}]. The limit $\beta \to \pi/2$ should be taken such that the Higgs-b-quark Yukawa coupling $h_b \equiv g_2 m_b/(\sqrt{2} m_W c_\beta)$ is fixed. (I have not put $s_\beta = 1$ in order to preserve the symmetry of the above formulae.) In the above results, $M_{\tilde{Q}}$ characterizes the common soft-supersymmetry breaking diagonal squark mass.

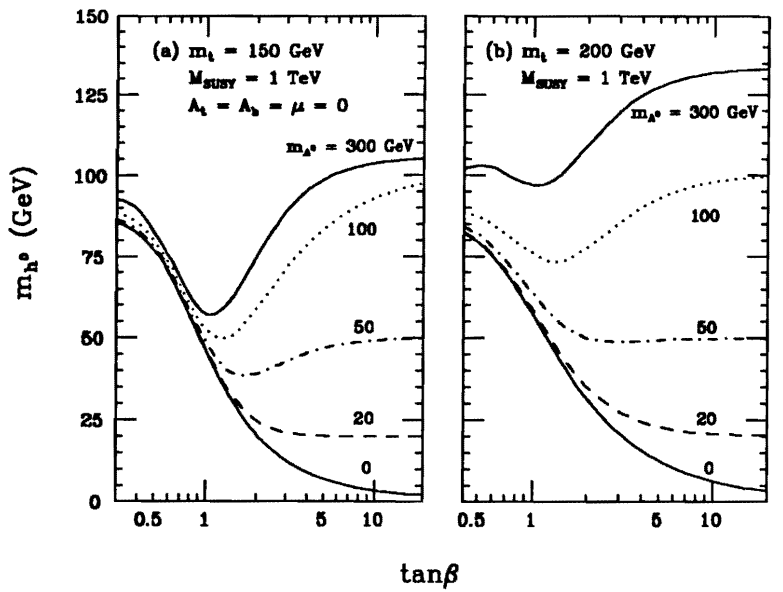

Fig. 9. RGE-improved Higgs mass m_{h^0} as a function of $\tan\beta$ for (a) $m_t = 150$ GeV and (b) $m_t = 200$ GeV. Various curves correspond to $m_{A^0} = 0$, 20, 50, 100 and 300 GeV as labeled in the figure. All A-parameters and μ are set equal to zero. The light CP-even Higgs mass varies very weakly with m_{A^0} for $m_{A^0} > 300$ GeV. Taken from ref. 54.

7. Numerical Results for MSSM Higgs Masses

In this section I shall briefly survey some of the numerical results for the radiatively corrected Higgs masses. Additional results can be found in ref. 54. Complementary work can be found in refs. [50,51,53,55–62]. In fig. 9(a) and (b) I plot the light CP-even Higgs mass as a function of $\tan\beta$ for $m_t = 150$ and 200 GeV for various choices of m_{A^0}. All A-parameters and μ are set equal to zero. The Higgs mass saturates at a maximum value, $m^{\max}_{h^0}$, when $\tan\beta$ and m_{A^0} become large. Furthermore, m_{h^0} converges to m_{A^0} in the limit $\tan\beta \to \infty$, as long as $m_{A^0} \le m^{\max}_{h^0}$. The reason for the h^0–A^0 mass degeneracy in this limit is easily understood. In the MSSM Higgs potential, the $\tan\beta \to \infty$ limit can be implemented by setting $m^2_{12} = 0$ while holding m_{A^0} fixed [see eq. (18)]. In this case, the model possesses an unbroken global U(1) symmetry which guarantees that $m_{h^0} = m_{A^0}$ to all orders in perturbation theory. That is, in this limit the radiative corrections to m_{h^0} vanish exactly. In the opposite case where $m_{A^0} \ge m^{\max}_{h^0}$, $m_{H^0} = m_{A^0}$ to all orders in perturbation theory,* while the radiative corrections to $m^2_{h^0}$ are substantial and grow with m^4_t. Note that for $m_{A^0} \gg m_Z$, the dominant m^4_t-contribution

* If both $A \neq 0$ and $\mu \neq 0$, then the U(1) symmetry is not exact and $m_{H^0} = m_{A^0}$ is violated, as shown explicitly in eq. (62).

to $m^2_{h^0}$ is independent of $\tan\beta$ [see eq. (57)]. As a result, at fixed $m_{A^0} > m^{\max}_{h^0}$, the radiatively corrected m_{h^0} will reach a maximum (minimum) at $\tan\beta \simeq \infty$ ($\tan\beta \simeq 1$), due to the tree-level behavior of $m^2_{h^0}$ on $\tan\beta$.

For fixed $\tan\beta$, m_{h^0} reaches its minimum value, $m^{\min}_{h^0}$, when $m_{A^0} \to 0$. In contrast to the tree-level behavior (where $m_{h^0} \leq m_{A^0}$), the Higgs mass does not vanish as $m_{A^0} \to 0$. Moreover, $m^{\min}_{h^0}$ increases as $\tan\beta$ decreases but exhibits only a moderate dependence on m_t and $M_{\rm SUSY}$. This behavior can be understood as follows. For $m_{A^0} \ll m_Z$ and for values of m_t and $M_{\rm SUSY}$ sufficiently large (say, $m_t \gtrsim 2m_Z s_\beta$ and $M_{\rm SUSY} \gtrsim 500$ GeV), the CP-even squared mass matrix [eq. (5)] is dominated by the matrix element $\mathcal{M}^2_{22}$ due to the m_t^4 dependence of λ_2. This yields

$$(m^2_{h^0})_{\min} \simeq \mathcal{M}^2_{11} - \frac{(\mathcal{M}^2_{12})^2}{\mathcal{M}^2_{22}} \approx m_Z^2 c_\beta^2 , \tag{63}$$

which is in good agreement with the results of fig. 9. One interesting consequence is that there exists a range of parameters for which the tree-level bound, $m_{h^0} \leq m_{A^0}$ is violated. In fact, the results of fig. 9 indicate that in the region of small $\tan\beta$ and small m_{A^0}, it is possible to have $m_{h^0} > 2m_{A^0}$, thereby allowing a new decay-mode $h^0 \to A^0A^0$ which is kinematically forbidden at tree-level.

One other difference between the tree-level prediction for m_{h^0} and the results of fig. 9 is noteworthy. From eq. (20), we see that for $\tan\beta = 1$, $m_{h^0} = 0$ at tree-level. The results of fig. 9 indicate that the radiative corrections to m_{h^0} are substantial for $\tan\beta = 1$, particularly when m_t is large. This is again a consequence of the $g^2 m_t^4 \ln(M^2_{\rm SUSY}/m_Z^2)$ enhancement of $\mathcal{M}^2_{22}$. The $\tan\beta = 1$ limit is analogous to the Coleman-Weinberg limit [66] of the Standard Model, in which the mass of the Higgs boson arises entirely from radiative corrections. However, in the Standard Model, the Coleman-Weinberg mechanism cannot be operative if $m_t \gtrsim m_W$ [67] (and in any case, the Higgs mass that arises from this mechanism cannot be larger than about 10 GeV, which is ruled out by the LEP Higgs search [12]). Clearly, no such restriction exists in the MSSM [68,58]. The difference lies in the large positive contribution to the Higgs squared mass from a loop of top squarks. From fig. 9(b), we see that for $m_t = 200$ GeV and $\tan\beta = 1$, a value of m_{h^0} as large as 100 GeV is possible. Thus, LEP cannot yet rule out the possibility that the mass of the lightest CP-even Higgs boson arises entirely from radiative corrections [58].

In the limit $m_{A^0} \to \infty$, the couplings of h^0 to gauge bosons and matter fields are identical to the Higgs couplings of the Standard Model so that the Higgs sector of the two models cannot be phenomenologically distinguished. However, supersymmetry does impose constraints on the quartic Higgs self-coupling at the scale $M_{\rm SUSY}$, and this influences the possible values of m_{h^0}. To illustrate this point, I have plotted in fig. 10 the range of allowed m_{h^0} in the case of large m_{A^0} (taken here to be $m_{A^0} = 300$ GeV). As noted above, the lower limit for m_{h^0} is

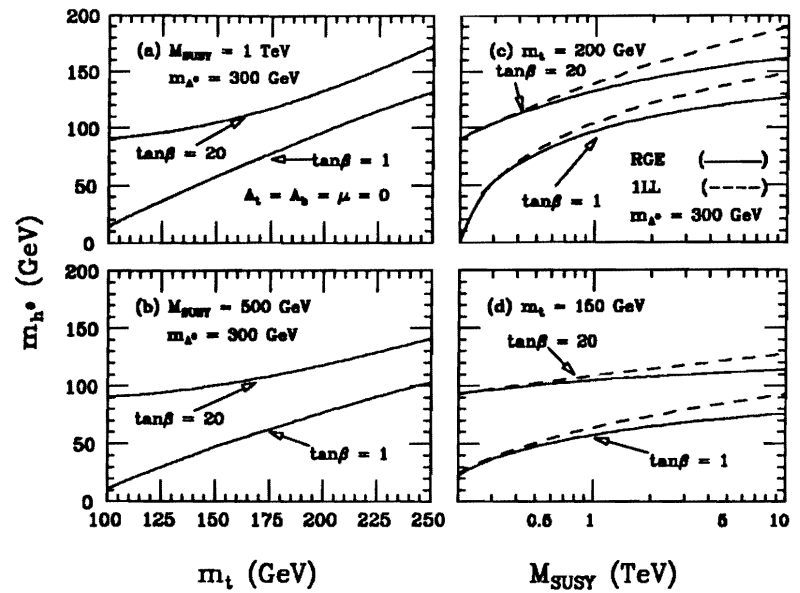

Fig. 10. The range of allowed Higgs masses for large m_{A^0} (in these plots, $m_{A^0} = 300$ GeV). The lower limit corresponds to $\tan\beta = 1$. The upper limit corresponds to the limit of large $\tan\beta$ (we take $\tan\beta = 20$). In (a) and (b) m_t is varied for $M_{\rm SUSY} = 1$ and 0.5 TeV, respectively. In (c) and (d) $M_{\rm SUSY}$ is varied and $m_t = 150$ and 200 GeV, respectively. The solid (dashed) curves in (c) and (d) correspond to the computation in which the RGEs are solved numerically (iteratively to one-loop order). Taken from ref. 54.

attained if $\tan\beta \simeq 1$ and the upper limit is attained in the limit of large $\tan\beta$ (taken to be $\tan\beta = 20$ in fig. 10).† Suppose the top quark mass is known and that h^0 is discovered with Standard Model couplings. If m_{h^0} does not lie in the allowed mass region displayed in fig. 10, we could conclude that the MSSM is ruled out. Fig. 10 also exhibits the sensitivity to the choice of $M_{\rm SUSY}$. The larger the value of $M_{\rm SUSY}$, the more significant the corrections to the Higgs mass due to full renormalization group improvement. In fig. 10(c) and (d), the dashed lines (labeled 1LL for one-loop leading-log) correspond to computing m_{h^0} by exactly diagonalizing the squared mass matrix given in eq. (51). The solid lines (denoted by RGE) are obtained by solving numerically the RGEs for the λ_i, inserting the results into eq. (5), and computing the eigenvalue of the lighter CP-even Higgs scalar. For $M_{\rm SUSY} = 1$ TeV, the largest discrepancy between the RGE and 1LL results occurs for large m_t and m_{A^0}. For example, for $\tan\beta = 1$, $m_{A^0} = 300$ GeV and $m_t = 200$ GeV, we find $(m_{h^0})_{\rm RGE} = 96.8$ GeV while $(m_{h^0})_{\rm 1LL} = 104.4$ GeV.

† A second maximum for m_{h^0} would arise for very small $\tan\beta$; however, this lies outside the permitted region indicated in figs. 1 and 2.

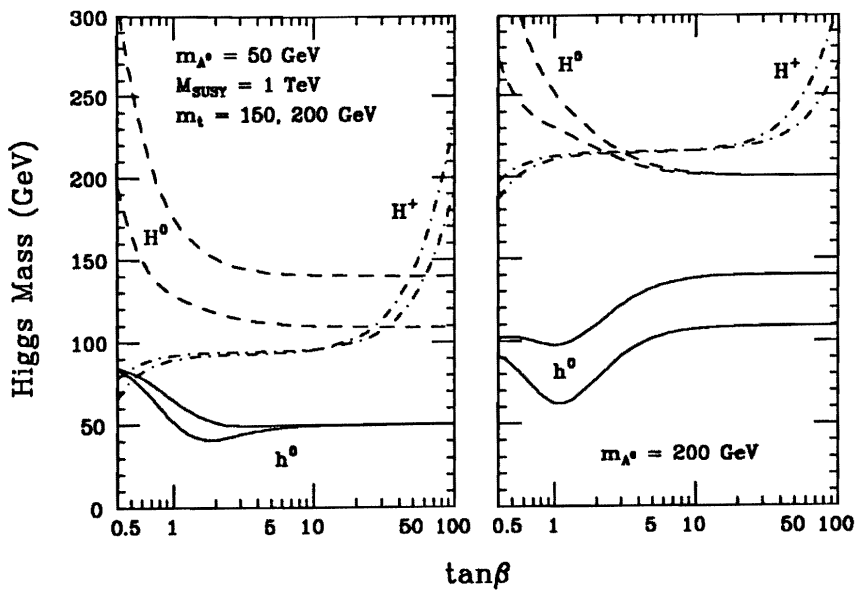

Fig. 11. The masses of h^0, H^0 and $H^\pm$ in the MSSM for $m_{A^0} = 50$ and 200 GeV. The neutral CP-even Higgs masses are obtained from a calculation that includes the leading-log one-loop radiative corrections [based on eq. (51)]. The charged Higgs mass is obtained from a similar calculation, but important non-leading logarithmic effects have also been included [59]. All supersymmetric masses are assumed to be roughly degenerate of order $M_{\rm SUSY} = 1$ TeV. The two curves for each Higgs mass shown correspond to $m_t = 150$ and 200 GeV. The larger neutral Higgs mass corresponds to the larger m_t choice. In the case of $H^\pm$, $m_{H^\pm}$ increases [decreases] with m_t for large [small] $\tan\beta$.

Values of $M_{\rm SUSY}$ much larger than 1 TeV would be in conflict with the philosophy of low-energy supersymmetry.

Let us now briefly consider the predictions of the one-loop radiatively corrected Higgs sector for the other physical Higgs bosons of the MSSM. In fig. 11, I plot the radiatively corrected MSSM Higgs masses as a function of $\tan\beta$ for $M_{\rm SUSY} = 1$ TeV and for two choices of m_t and m_{A^0}. (As above, all A and μ parameters are set to zero.) The neutral Higgs masses have been obtained by diagonalizing eq. (51). Full RGE-improvement, which is not included in fig. 11, would change these results by no more than about 5%. In the case of the charged Higgs mass, important non-leading logarithmic contributions have also been included, as described in ref. 59. Note that the tree-level bound $m_{H^\pm} \geq m_W$ can be violated, but only if $\tan\beta \lesssim 0.5$ and m_{A^0} is small. The small $\tan\beta$ region corresponds to an enhanced Higgs-top quark Yukawa coupling. This also explains the increase of m_{H^0} in this region, which is being controlled by the m_t^4/s_β^2 factor in $\mathcal{M}_{22}^2$ [eq. (51)]. Of course, this

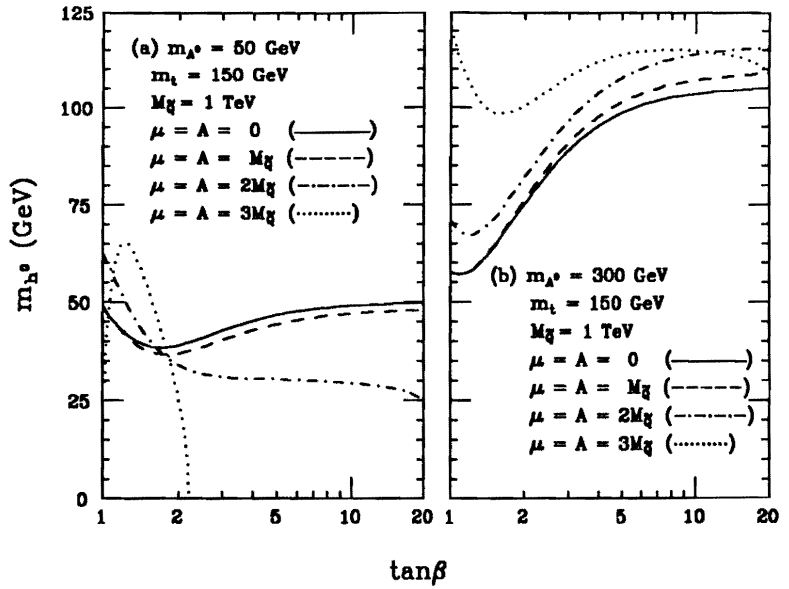

Fig. 12. The neutral Higgs mass m_{h^0} as a function of $\tan\beta$ for (a) $m_{A^0} = 50$ GeV and (b) $m_{A^0} = 300$ GeV, for $m_t = 150$ GeV and $M_{\tilde{Q}} = M_{\rm SUSY} = 1$ TeV. All A-parameters are taken to be equal ($A = A_t = A_b$); the four contours shown correspond to $\mu = A = 0$, 1, 2 and 3 TeV, respectively. Taken from ref. 54.

same factor is responsible for the violation of the bound $m_{h^0} \leq m_Z$ as described in section 5. Indeed, for $M_{\rm SUSY} = 1$ TeV, $m_t = 200$ GeV, and $m_{A^0} \gtrsim 200$ GeV, one sees that $m_{h^0} > m_Z$ independent of the value of $\tan\beta$. Thus, there is a non-negligible region of parameter space in which the h^0 is kinematically inaccessible to LEP-II (running at $\sqrt{s} \leq 200$ GeV).

The numerical results described above can be substantially modified if squark mixing effects are large. In this case, the A-parameters and μ are no longer zero, and non-leading-log contributions to the neutral Higgs masses [*e.g.*, see eqs. (61) and (62)] can be important. In fig. 12, the Higgs mass m_{h^0} is plotted as a function of $\tan\beta$ for $m_t = 150$ GeV and for two choices of m_{A^0}. All A-parameters are taken to be equal; the four curves shown correspond to $\mu = A = 0, 1, 2$ and 3 TeV, respectively. The behavior of m_{h^0} at large values of $\tan\beta$ is noteworthy: for $m_{A^0} \lesssim m_Z$, one sees that m_{h^0} decreases monotonically with A. In contrast, in the case $m_{A^0} \gtrsim m_Z$ and large $\tan\beta$, m_{h^0} initially increases, reaches a maximum and then falls off again. Both properties can be understood from eqs. (61) and (62). The consistency of the supersymmetric model does not permit arbitrarily large squark mixing. For example, for $A_t \gtrsim 3M_{\rm SUSY}$, one would find either one eigenvalue of the top squark squared mass matrix driven negative and/or a new global minimum of

the scalar potential that violates the SU(3) color gauge symmetry [69]. Of course, either result would be phenomenologically unacceptable.

8. Implications of the Radiatively Corrected Higgs Sector

Using the results of section 6, one can obtain the leading logarithmic corrections to the various Higgs couplings, and proceed to investigate Higgs phenomenology in detail [70]. Here, I shall describe the procedure used to obtain the Higgs couplings and briefly indicate some of the consequences. To obtain radiatively corrected couplings which are accurate in the leading logarithmic approximation, it is sufficient to use the tree-level couplings in which the parameters are taken to be running parameters evaluated at the electroweak scale. First, I remind the reader that $\tan\beta$ and m_{A^0} are input parameters. Next, we obtain the CP-even Higgs mixing angle α by diagonalizing the radiatively corrected CP-even Higgs mass matrix. With the angle α in hand one may compute, for example, $\cos(\beta-\alpha)$ and $\sin\alpha$. These results can be used to obtain the Higgs couplings to gauge bosons [eq. (14)] and fermions [eq. (15)]. Finally, the Higgs self-couplings [see Appendix A] are obtained by making use of the λ_i evaluated at the electroweak scale. The end result is a complete set of Higgs boson decay widths and branching ratios that include leading-log radiative corrections.

The Higgs production cross-section in a two-Higgs-doublet model via the process $e^+e^- \to Z \to ZH^0(Zh^0)$ is suppressed by a factor $\cos^2(\beta-\alpha)$ $[\sin^2(\beta-\alpha)]$ as compared to the corresponding cross-sections in the Standard Model. In fig. 13 I plot $\cos^2(\beta-\alpha)$ as a function of m_{A^0} for $\tan\beta = 0.5, 1, 2$ and 20, for $A_t = A_b = \mu = 0$, $M_{\rm SUSY} = 1$ TeV and two choices of m_t. The behavior is similar to that of the tree-level result: (i) for $m_{A^0} \ll m_Z$ and $\tan\beta \gg 1$, $\cos^2(\beta-\alpha) \simeq 1$, and (ii) for $m_{A^0} \gtrsim 2m_Z$, $\sin^2(\beta-\alpha) \simeq 1$. The fact that $\cos^2(\beta-\alpha) \to 0$ as m_{A^0} becomes large is expected since for large m_{A^0}, all heavy Higgs states decouple, while the h^0ZZ coupling [which is proportional to $\sin(\beta-\alpha)$] approaches its Standard Model value. Nevertheless, it is interesting to note that $\cos^2(\beta-\alpha)$ approaches 0 more slowly as m_t increases (*i.e.*, as the radiative corrections become more significant).

When radiative corrections have been incorporated, new possibilities arise which did not exist at tree-level. One example, mentioned in section 6, is the possibility of the decay $h^0 \to A^0A^0$, which is kinematically forbidden at tree-level but allowed for some range of MSSM parameters [61,71]. We can obtain the complete one-loop leading-log expression for the $h^0A^0A^0$ coupling (assuming $m_{A^0} \lesssim m_Z$) by inserting the one-loop leading-log formulae for the λ_i into eq. (A.1) [71]

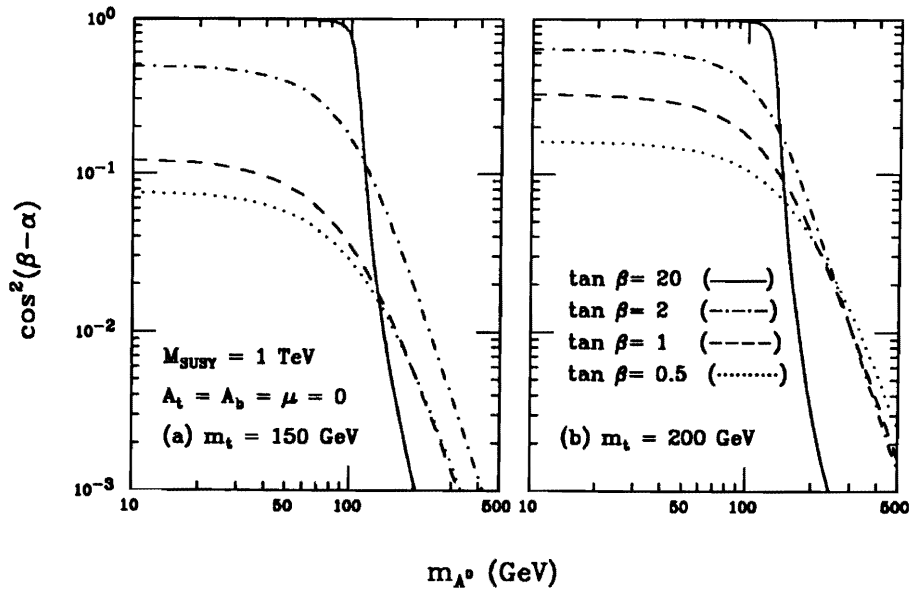

Fig. 13. The factor $\cos^2(\beta-\alpha)$ as a function of m_{A^0} for $\tan\beta = 0.5, 1, 2$ and 20 (dotted, dashed, dot-dashed and solid curves, respectively). Results are presented for $M_{\rm SUSY} = 1$ TeV. We consider the case of (a) $m_t = 150$ GeV and (b) $m_t = 200$ GeV. Taken from ref. 54.

$$\frac{g_{h^0A^0A^0}}{gm_Z/2c_W} = -c_{2\beta}s_{\beta+\alpha}\left\{1+\frac{g^2}{96\pi^2c_W^2}\left[P_t\ln\left(\frac{M_{\rm SUSY}^2}{m_t^2}\right)+P_f\ln\left(\frac{M_{\rm SUSY}^2}{m_Z^2}\right)\right]\right\}$$
$$+\frac{g^2N_c}{16\pi^2m_W^2m_Z^2}\left\{\left[\frac{s_\alpha s_\beta^2}{c_\beta^3}(2m_b^4-m_b^2m_Z^2c_\beta^2)-\frac{(c_\alpha s_\beta^3-s_\alpha c_\beta^3)}{2c_\beta^2}m_b^2m_Z^2\right]\ln\left(\frac{M_{\rm SUSY}^2}{m_Z^2}\right)\right.$$
$$\left.-\left[\frac{c_\alpha c_\beta^2}{s_\beta^3}(2m_t^4-m_t^2m_Z^2s_\beta^2)+\frac{(c_\alpha s_\beta^3-s_\alpha c_\beta^3)}{2s_\beta^2}m_t^2m_Z^2\right]\ln\left(\frac{M_{\rm SUSY}^2}{m_t^2}\right)\right\}$$
$$-\frac{g^2}{192\pi^2c_W^2}\left[s_{2\beta}c_{\beta+\alpha}(P_{2H}+P_g)-2(c_\alpha s_\beta^3-s_\alpha c_\beta^3)(P'_{2H}+P'_g)\right]\ln\left(\frac{M_{\rm SUSY}^2}{m_Z^2}\right). \tag{64}$$

Once kinematically allowed, $h^0 \to A^0A^0$ is almost certainly the dominant decay mode as shown in fig. 14. These results indicate the importance of the search for $h^0 \to A^0A^0$ at LEP. As m_{A^0} increases beyond 30 GeV, the region of parameter space where this decay is permitted quickly shrinks.

Recent Higgs searches at LEP have begun to incorporate the most important leading-log radiative corrections into their analyses (see, *e.g.*, ref. [14]). However,

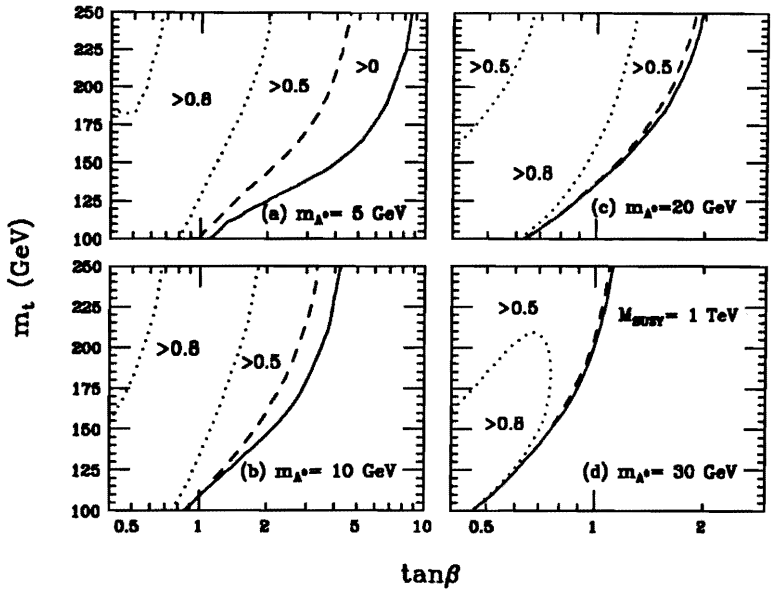

Fig. 14. Regions of nonvanishing $BR(h^0 \to A^0A^0)$ for $m_{A^0} = 5, 10, 20$ and 30 GeV. To the right of the solid curves, $m_{h^0} < 2m_{A^0}$, and the decay $h^0 \to A^0A^0$ is kinematically forbidden. To the left of the dashed curve, $BR(h^0 \to A^0A^0) \geq 0.5$ and between the dotted curves, $BR(h^0 \to A^0A^0) \geq 0.8$. $M_{\rm SUSY} = 1$ TeV in all four graphs. Taken from ref. 71.

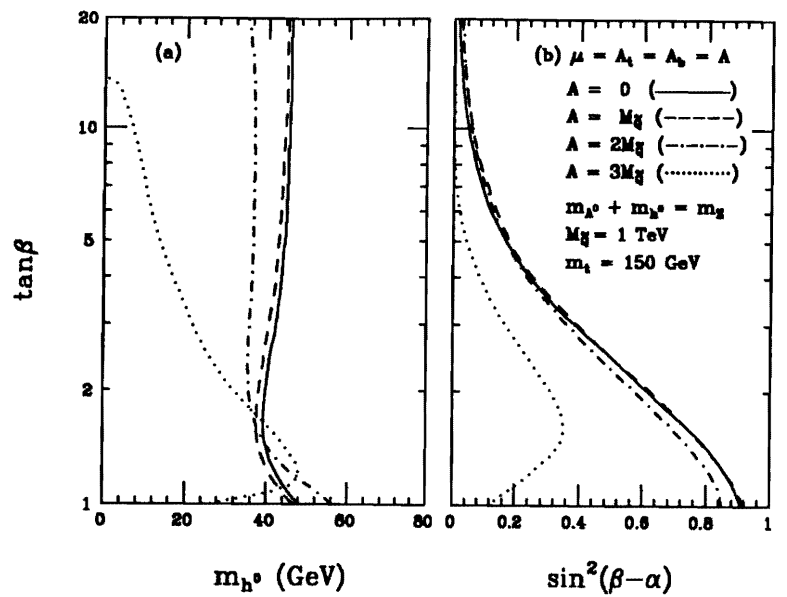

Fig. 15. As a function of $\tan\beta$, we plot (a) the neutral Higgs mass m_{h^0} and (b) the factor $\sin^2(\beta-\alpha)$ for $m_t = 150$ GeV and $M_{\tilde{Q}} = M_{\rm SUSY} = 1$ TeV. All A-parameters are taken to be equal ($A = A_t = A_b$); the four curves shown correspond to $\mu = A = 0, 1, 2$ and 3 TeV, respectively. The sum $m_{A^0} + m_{h^0} = m_Z$ is kept fixed in both plots. Taken from ref. [54].

if squark mixing effects are large, then important non-leading-log effects cannot be neglected, as discussed at the end of section 6 [15]. In fig. 15 I plot the Higgs mass m_{h^0} and the factor $\sin^2(\beta-\alpha)$ as functions of $\tan\beta$ for $m_t = 150$ GeV and $M_{\rm SUSY} = 1$ TeV. I have fixed the sum $m_{A^0} + m_{h^0} = m_Z$ in both plots in order to bound m_{h^0} while keeping $Z \to A^0h^0$ kinematically forbidden. Fig. 15(a) displays contours of fixed $m_{A^0} + m_{h^0} = m_Z$. To the left (right) of these contours, $Z \to A^0h^0$ is kinematically allowed (forbidden). In fig. 15(b) one sees that the decay $Z \to Z^*h^0$, with a rate proportional to $\sin^2(\beta-\alpha)$, can be sufficiently suppressed in the large $\tan\beta$ regime to escape detection. On the other hand, the rate for $Z \to A^0h^0$ is proportional to $\cos^2(\beta-\alpha)$ which is near unity for large $\tan\beta$ and $m_{A^0} \lesssim m_Z$. Thus, $Z \to A^0h^0$ would be observed in this regime unless it is kinematically forbidden. Thus, in the absence of the Higgs discovery at LEP, one can conclude that the parameter regions to the left of the respective curves (for various choices of $\mu = A$) shown in fig. 15(a) are excluded. On the other hand, at large $\tan\beta$, the parameter regime to the right of the respective curves cannot be ruled out based on current LEP data. In particular, for large $\mu = A$ (and for large $\tan\beta$), the true experimental lower limit on m_{h^0} [*i.e.*, the dotted curve of fig. 15(a)] can be significantly lower than the quoted Higgs mass limits of the LEP

detector collaborations [13-14].

For the heavier Higgs states, there are many possible final state decay modes. The various branching ratios are complicated functions of the MSSM parameter space [72]. Plots of the branching ratios of the MSSM Higgs bosons, with all one-loop leading log corrections included, can be found in J.F. Gunion's contribution to this Volume. These plots indicate a rich phenomenology for Higgs searches at future colliders [72,73]. Although the possibility of a Higgs discovery at LEP still remains, the effects of the radiative corrections (particularly if m_t is near the upper end of its expected range) suggest that the success of the Higgs Hunt must await the supercollider era. Presumably, the SSC and LHC will uncover direct evidence for supersymmetric particles, if low-energy supersymmetry exists. In this case, the details of the Higgs sector will contain crucial information regarding the structure of the theory—the mechanism of electroweak symmetry breaking and the nature of the TeV scale physics that lies beyond the Standard Model.

APPENDIX A: Three-Higgs Vertices in the Two-Higgs Doublet Model

In this Appendix, I list the Feynman rules for the 3-point Higgs interaction in the most general (nonsupersymmetric) two-Higgs doublet extension of the Standard Model, assuming that the Higgs sector conserves CP. The Feynman rule for the ABC vertex is denoted by ig_{ABC}. For completeness, R-gauge Feynman rules involving the Goldstone bosons ($G^{\pm}$ and G^0) are also listed.

Interactions involving physical Higgs bosons depend in detail on the parameters of the Higgs potential specified in eq. (1).

$$
\begin{aligned}
g_{h^0A^0A^0} &= \frac{2m_W}{g}\big[\lambda_1 s_\beta^2 c_\beta s_\alpha - \lambda_2 c_\beta^2 s_\beta c_\alpha - \tilde{\lambda}_3(s_\beta^3 c_\alpha - c_\beta^3 s_\alpha) + 2\lambda_5 s_{\beta-\alpha} \\
&\quad - \lambda_6 s_\beta\big(c_\beta s_{\alpha+\beta} + s_\alpha c_{2\beta}\big) - \lambda_7 c_\beta\big(c_\alpha c_{2\beta} - s_\beta s_{\alpha+\beta}\big)\big]\,, \\
g_{H^0A^0A^0} &= \frac{-2m_W}{g}\big[\lambda_1 s_\beta^2 c_\beta c_\alpha + \lambda_2 c_\beta^2 s_\beta s_\alpha + \tilde{\lambda}_3(s_\beta^3 s_\alpha + c_\beta^3 c_\alpha) - 2\lambda_5 c_{\beta-\alpha} \\
&\quad - \lambda_6 s_\beta\big(c_\beta c_{\alpha+\beta} + c_\alpha c_{2\beta}\big) + \lambda_7 c_\beta\big(s_\beta c_{\alpha+\beta} + s_\alpha c_{2\beta}\big)\big]\,, \\
g_{h^0H^0H^0} &= \frac{6m_W}{g}\big[\lambda_1 c_\alpha^2 c_\beta s_\alpha - \lambda_2 s_\alpha^2 s_\beta c_\alpha + \tilde{\lambda}_3(s_\alpha^3 c_\beta - c_\alpha^3 s_\beta + \tfrac{2}{3} s_{\beta-\alpha}) \\
&\quad - \lambda_6 c_\alpha\big(c_\beta c_{2\alpha} - s_\alpha s_{\alpha+\beta}\big) - \lambda_7 c_\alpha\big(s_\beta c_{2\alpha} + c_\alpha s_{\alpha+\beta}\big)\big]\,, \\
g_{H^0h^0h^0} &= \frac{-6m_W}{g}\big[\lambda_1 s_\alpha^2 c_\beta c_\alpha + \lambda_2 c_\alpha^2 s_\beta s_\alpha + \tilde{\lambda}_3(s_\alpha^3 s_\beta + c_\alpha^3 c_\beta - \tfrac{2}{3} c_{\beta-\alpha}) \\
&\quad - \lambda_6 s_\alpha\big(c_\beta c_{2\alpha} + c_\alpha c_{\alpha+\beta}\big) + \lambda_7 c_\alpha\big(s_\beta c_{2\alpha} + s_\alpha c_{\alpha+\beta}\big)\big]\,, \qquad \text{(A.1)} \\
g_{h^0h^0h^0} &= \frac{6m_W}{g}\big[\lambda_1 s_\alpha^3 c_\beta - \lambda_2 c_\alpha^3 s_\beta + \tilde{\lambda}_3 s_\alpha c_\alpha c_{\alpha+\beta} \\
&\quad - \lambda_6 s_\alpha^2\big(3c_\alpha c_\beta - s_\alpha s_\beta\big) + \lambda_7 c_\alpha^2\big(3s_\alpha s_\beta - c_\alpha c_\beta\big)\big]\,, \\
g_{H^0H^0H^0} &= \frac{-6m_W}{g}\big[\lambda_1 c_\alpha^3 c_\beta + \lambda_2 s_\alpha^3 s_\beta + \tilde{\lambda}_3 s_\alpha c_\alpha s_{\alpha+\beta} \\
&\quad + \lambda_6 c_\alpha^2\big(3s_\alpha c_\beta + c_\alpha s_\beta\big) + \lambda_7 s_\alpha^2\big(3c_\alpha s_\beta + s_\alpha c_\beta\big)\big]\,, \\
g_{h^0H^+H^-} &= g_{h^0A^0A^0} - \frac{2m_W}{g}(\lambda_5 - \lambda_4)s_{\beta-\alpha}\,, \\
g_{H^0H^+H^-} &= g_{H^0A^0A^0} - \frac{2m_W}{g}(\lambda_5 - \lambda_4)c_{\beta-\alpha}\,,
\end{aligned}
$$

where I have used the notation

$$\tilde{\lambda}_3 \equiv \lambda_3 + \lambda_4 + \lambda_5\,. \qquad \text{(A.2)}$$

It is interesting to note that couplings of the charged Higgs bosons satisfy relations analogous to that of $m_{H^\pm}$ given in eq. (4).

Feynman rules for three-point Higgs vertices that involve Goldstone bosons assume much simpler forms

$$
\begin{aligned}
g_{h^0G^0G^0} &= \frac{-g}{2m_W} m_{h^0}^2 \sin(\beta-\alpha)\,, \\
g_{H^0G^0G^0} &= \frac{-g}{2m_W} m_{H^0}^2 \cos(\beta-\alpha)\,, \\
g_{h^0G^+G^-} &= g_{h^0G^0G^0}\,, \\
g_{H^0G^+G^-} &= g_{H^0G^0G^0}\,, \\
g_{h^0A^0G^0} &= \frac{-g}{2m_W}(m_Z^2 - m_{H^0}^2)\cos(\beta-\alpha)\,, \qquad \text{(A.3)} \\
g_{H^0A^0G^0} &= \frac{g}{2m_W}(m_Z^2 - m_{h^0}^2)\sin(\beta-\alpha)\,, \\
g_{h^0H^\pm G^\mp} &= \frac{g}{2m_W}(m_{H^\pm}^2 - m_{h^0}^2)\cos(\beta-\alpha)\,, \\
g_{H^0H^\pm G^\mp} &= \frac{-g}{2m_W}(m_{H^\pm}^2 - m_{H^0}^2)\sin(\beta-\alpha)\,, \\
g_{A^0H^\pm G^\mp} &= \frac{\pm g}{2m_W}(m_{H^\pm}^2 - m_{A^0}^2)\,.
\end{aligned}
$$

In the rule for the $A^0H^\pm G^\mp$ vertex, the sign corresponds to $H^\pm$ entering the vertex and $G^\pm$ leaving the vertex.

One can easily check that if tree-level MSSM relations are imposed on the λ_i, Higgs masses, and angles α and β, one recovers the MSSM Feynman rules listed in Appendix A of ref. 1.

APPENDIX B: Renormalization Group Equations

In this Appendix, I have collected the one-loop renormalization group equations (RGEs) that are needed in the analysis presented in this paper [74,17,54]. Schematically, the RGEs at one-loop take the form

$$\frac{dp_i}{dt} = \beta_i(p_1, p_2, ..), \qquad \text{where } t \equiv \ln \mu^2 , \tag{B.1}$$

where μ is the energy scale, and the parameters p_i stand for the Higgs boson self-couplings λ_i ($i = 1 \ldots 7$), the squared Yukawa couplings h_f^2 ($f = t$, b and τ; the two lighter generations can be neglected), and the squared gauge couplings g_j^2 (j =3, 2, 1) corresponding to SU(3)×SU(2)×U(1) respectively. The g_j are normalized such that they are equal at the grand unification scale. It is also convenient to define

$$g \equiv g_2 , \qquad g' \equiv \sqrt{\tfrac{3}{5}} g_1 , \tag{B.2}$$

where g and g' are normalized in the usual way for low-energy electroweak physics, *i.e.* $\tan\theta_W = g'/g$.

I now list the β-functions required for the analysis presented in this paper. Two cases will be given, depending on whether μ is above or below the scale of supersymmetry breaking, $M_{\rm SUSY}$.

1. $\mu > M_{\rm SUSY}$

$$\begin{aligned}
\beta_{h_t^2} &= \frac{h_t^2}{16\pi^2}\left[6h_t^2 + h_b^2 - \tfrac{16}{3}g_3^2 - 3g^2 - \tfrac{13}{9}g'^2\right] \\
\beta_{h_b^2} &= \frac{h_b^2}{16\pi^2}\left[6h_b^2 + h_t^2 + h_\tau^2 - \tfrac{16}{3}g_3^2 - 3g^2 - \tfrac{7}{9}g'^2\right] \\
\beta_{h_\tau^2} &= \frac{h_\tau^2}{16\pi^2}\left[4h_\tau^2 + 3h_b^2 - 3g^2 - 3g'^2\right] \\
\beta_{g'^2} &= \frac{g'^4}{48\pi^2}\left[10N_g + \tfrac{3}{2}N_H\right] \\
\beta_{g^2} &= \frac{g^4}{48\pi^2}\left[6N_g + \tfrac{3}{2}N_H - 18\right] \\
\beta_{g_3^2} &= \frac{g_3^4}{48\pi^2}\left[6N_g - 27\right].
\end{aligned} \tag{B.3}$$

Here $N_g = 3$ is the number of generations, $N_H = 2$ is the number of scalar doublets, and the Higgs-fermion Yukawa couplings are given by

$$\begin{aligned}
h_t &= \frac{g m_t}{\sqrt{2} m_W \sin\beta}, \\
h_{d_i} &= \frac{g m_d}{\sqrt{2} m_W \cos\beta}, \qquad (d_i = b, \tau).
\end{aligned} \tag{B.4}$$

2. $\mu < M_{\rm SUSY}$

$$\begin{aligned}
\beta_{h_t^2} &= \frac{h_t^2}{16\pi^2}\left[\tfrac{9}{2}h_t^2 + \tfrac{1}{2}h_b^2 - 8g_3^2 - \tfrac{9}{4}g^2 - \tfrac{17}{12}g'^2\right] \\
\beta_{h_b^2} &= \frac{h_b^2}{16\pi^2}\left[\tfrac{9}{2}h_b^2 + \tfrac{1}{2}h_t^2 + h_\tau^2 - 8g_3^2 - \tfrac{9}{4}g^2 - \tfrac{5}{12}g'^2\right] \\
\beta_{h_\tau^2} &= \frac{h_\tau^2}{16\pi^2}\left[\tfrac{5}{2}h_\tau^2 + 3h_b^2 - \tfrac{9}{4}g^2 - \tfrac{15}{4}g'^2\right] \\
\beta_{g'^2} &= \frac{g'^4}{48\pi^2}\left[\tfrac{20}{3}N_g + \tfrac{1}{2}N_H\right] \\
\beta_{g^2} &= \frac{g^4}{48\pi^2}\left[4N_g + \tfrac{1}{2}N_H - 22\right] \\
\beta_{g_3^2} &= \frac{g_3^4}{48\pi^2}\left[4N_g - 33\right].
\end{aligned} \tag{B.5}$$

The notation is the same as in the previous case. Moreover, in writing down the RGEs for the Higgs-fermion Yukawa couplings, I have assumed that the Higgs-fermion interaction is the same as in the MSSM; namely, Φ_1 [Φ_2] couples exclusively to down-type [up-type] fermions.

Finally, I list the RGEs for the Higgs self-couplings of the general two-Higgs doublet model (with the Higgs-fermion couplings as specified above). First, I need to define the anomalous dimensions of the two Higgs fields:

$$\begin{aligned}
\gamma_1 &= \frac{1}{64\pi^2}\left[9g^2 + 3g'^2 - 4\sum_i N_{ci} h_{d_i}^2\right], \\
\gamma_2 &= \frac{1}{64\pi^2}\left[9g^2 + 3g'^2 - 4\sum_i N_{ci} h_{u_i}^2\right],
\end{aligned} \tag{B.6}$$

where the sum over i is taken over three generations of quarks (with $N_c = 3$) and

leptons (with $N_c = 1$). The β-functions for the Higgs self-couplings in the general CP-conserving non-supersymmetric two-Higgs-doublet model (with the Higgs-fermion couplings as specified in section 2) are given by

$$\beta_{\lambda_1} = \frac{1}{16\pi^2}\Big\{6\lambda_1^2 + 2\lambda_3^2 + 2\lambda_3\lambda_4 + \lambda_4^2 + \lambda_5^2 + 12\lambda_6^2 + \tfrac{3}{8}\left[2g^4 + (g^2+g'^2)^2\right] - 2\sum_i N_{ci} h_{d_i}^4\Big\} - 2\lambda_1\gamma_1$$

$$\beta_{\lambda_2} = \frac{1}{16\pi^2}\Big\{6\lambda_2^2 + 2\lambda_3^2 + 2\lambda_3\lambda_4 + \lambda_4^2 + \lambda_5^2 + 12\lambda_7^2 + \tfrac{3}{8}\left[2g^4 + (g^2+g'^2)^2\right] - 2\sum_i N_{ci} h_{u_i}^4\Big\} - 2\lambda_2\gamma_2$$

$$\beta_{\lambda_3} = \frac{1}{16\pi^2}\Big\{(\lambda_1+\lambda_2)(3\lambda_3+\lambda_4) + 2\lambda_3^2 + \lambda_4^2 + \lambda_5^2 + 2\lambda_6^2 + 2\lambda_7^2 + 8\lambda_6\lambda_7 + \tfrac{3}{8}\left[2g^4 + (g^2-g'^2)^2\right] - 2\sum_i N_{ci} h_{u_i}^2 h_{d_i}^2\Big\} - \lambda_3(\gamma_1+\gamma_2)$$

$$\beta_{\lambda_4} = \frac{1}{16\pi^2}\Big[\lambda_4(\lambda_1+\lambda_2+4\lambda_3+2\lambda_4) + 4\lambda_5^2 + 5\lambda_6^2 + 5\lambda_7^2 + 2\lambda_6\lambda_7 + \tfrac{3}{2}g^2g'^2 + 2\sum_i N_{ci} h_{u_i}^2 h_{d_i}^2\Big] - \lambda_4(\gamma_1+\gamma_2)$$

$$\beta_{\lambda_5} = \frac{1}{16\pi^2}\Big[\lambda_5(\lambda_1+\lambda_2+4\lambda_3+6\lambda_4) + 5(\lambda_6^2+\lambda_7^2) + 2\lambda_6\lambda_7\Big] - \lambda_5(\gamma_1+\gamma_2)$$

$$\beta_{\lambda_6} = \frac{1}{16\pi^2}\Big[\lambda_6(6\lambda_1+3\lambda_3+4\lambda_4+5\lambda_5) + \lambda_7(3\lambda_3+2\lambda_4+\lambda_5)\Big] - \tfrac{1}{2}\lambda_6(3\gamma_1+\gamma_2)$$

$$\beta_{\lambda_7} = \frac{1}{16\pi^2}\Big[\lambda_7(6\lambda_2+3\lambda_3+4\lambda_4+5\lambda_5) + \lambda_6(3\lambda_3+2\lambda_4+\lambda_5)\Big] - \tfrac{1}{2}\lambda_7(\gamma_1+3\gamma_2)\,. \tag{B.7}$$

APPENDIX C: MSSM Higgs Sector Contributions to the S, T and U Parameters

In this Appendix, I record the exact one-loop contributions of the MSSM Higgs bosons to δS, δT and δU [see eq. (32)]. These contributions are defined relative to the Standard Model in which the Standard Model Higgs boson mass is taken equal to m_{h^0} [38]. First, for δS and δU I find

$$\delta S = \frac{1}{\pi m_Z^2}\Big\{\sin^2(\beta-\alpha)\mathcal{B}_{22}(m_Z^2; m_{H^0}^2, m_{A^0}^2) - \mathcal{B}_{22}(m_Z^2; m_{H^\pm}^2, m_{H^\pm}^2) + \cos^2(\beta-\alpha)\Big[\mathcal{B}_{22}(m_Z^2; m_{h^0}^2, m_{A^0}^2) + \mathcal{B}_{22}(m_Z^2; m_Z^2, m_{H^0}^2) - \mathcal{B}_{22}(m_Z^2; m_Z^2, m_{h^0}^2) - m_Z^2\mathcal{B}_0(m_Z^2; m_Z^2, m_{H^0}^2) + m_Z^2\mathcal{B}_0(m_Z^2; m_Z^2, m_{h^0}^2)\Big]\Big\}.$$

$$\delta U = -\delta S + \frac{1}{\pi m_Z^2}\Big\{\mathcal{B}_{22}(m_W^2; m_{A^0}^2, m_{H^\pm}^2) - 2\mathcal{B}_{22}(m_W^2; m_{H^\pm}^2, m_{H^\pm}^2) + \sin^2(\beta-\alpha)\mathcal{B}_{22}(m_W^2; m_{H^0}^2, m_{H^\pm}^2) + \cos^2(\beta-\alpha)\Big[\mathcal{B}_{22}(m_W^2; m_{h^0}^2, m_{H^\pm}^2) + \mathcal{B}_{22}(m_W^2; m_W^2, m_{H^0}^2) - \mathcal{B}_{22}(m_W^2; m_W^2, m_{h^0}^2) - m_W^2\mathcal{B}_0(m_W^2; m_W^2, m_{H^0}^2) + m_W^2\mathcal{B}_0(m_W^2; m_W^2, m_{h^0}^2)\Big]\Big\}. \tag{C.1}$$

The following notation has been introduced for the various loop integrals

$$\mathcal{B}_{22}(q^2; m_1^2, m_2^2) \equiv B_{22}(q^2; m_1^2, m_2^2) - B_{22}(0; m_1^2, m_2^2)\,, \tag{C.2}$$

$$\mathcal{B}_0(q^2; m_1^2, m_2^2) \equiv B_0(q^2; m_1^2, m_2^2) - B_0(0; m_1^2, m_2^2)\,, \tag{C.3}$$

and B_{22} and B_0 are defined according to ref. [75] (up to an overall sign in some cases since I use the Bjorken and Drell metric [76]). Explicitly,

$$B_{22}(q^2; m_1^2, m_2^2) = \tfrac{1}{4}(\Delta+1)\left[m_1^2 + m_2^2 - \tfrac{1}{3}q^2\right] - \tfrac{1}{2}\int_0^1 dx\, X\ln(X - i\epsilon)\,, \tag{C.4}$$

$$B_0(q^2; m_1^2, m_2^2) = \Delta - \int_0^1 dx\, \ln(X - i\epsilon)\,, \tag{C.5}$$

where

$$X \equiv m_1^2 x + m_2^2(1-x) - q^2 x(1-x) \tag{C.6}$$

and Δ is the regulator of dimensional regularization defined by

$$\Delta = \frac{2}{4-n} + \ln(4\pi) + \gamma, \tag{C.7}$$

n is the number of space-time dimensions and γ is Euler's constant. Of course, in the calculation of physical observables, terms proportional to Δ must exactly cancel. The following two relations are particularly useful:

$$4B_{22}(0; m_1^2, m_2^2) = F(m_1^2, m_2^2) + A_0(m_1^2) + A_0(m_2^2), \tag{C.8}$$

$$B_0(0; m_1^2, m_2^2) = \frac{A_0(m_1^2) - A_0(m_2^2)}{m_1^2 - m_2^2}, \tag{C.9}$$

where

$$F(m_1^2, m_2^2) \equiv \tfrac{1}{2}(m_1^2 + m_2^2) - \frac{m_1^2 m_2^2}{m_1^2 - m_2^2} \ln\left(\frac{m_1^2}{m_2^2}\right), \tag{C.10}$$

$$A_0(m^2) \equiv m^2(\Delta + 1 - \ln m^2). \tag{C.11}$$

Finally, consider $\delta\rho = \alpha\delta T$. I find:

$$\begin{aligned}\delta T = \frac{1}{16\pi m_W^2 s_W^2}\Big\{ & F(m_{H^\pm}^2, m_{A^0}^2) + \sin^2(\beta-\alpha)\left[F(m_{H^\pm}^2, m_{H^0}^2) - F(m_{A^0}^2, m_{H^0}^2)\right] \\ & + \cos^2(\beta-\alpha)\left[F(m_{H^\pm}^2, m_{h^0}^2) - F(m_{A^0}^2, m_{h^0}^2) + F(m_W^2, m_{H^0}^2)\right. \\ & \left. - F(m_W^2, m_{h^0}^2) - F(m_Z^2, m_{H^0}^2) + F(m_Z^2, m_{h^0}^2)\right] \\ & + 4m_Z^2\left[B_0(0; m_Z^2, m_{H^0}^2) - B_0(0; m_Z^2, m_{h^0}^2)\right] \\ & - 4m_W^2\left[B_0(0; m_W^2, m_{H^0}^2) - B_0(0; m_W^2, m_{h^0}^2)\right]\Big\},\end{aligned} \tag{C.12}$$

where $s_W \equiv \sin\theta_W$.

Note that these expressions for δS, δT and δU are valid for an arbitrary two-Higgs doublet extension of the Standard Model [39-41]. In the MSSM, tree-level relations exist among the Higgs masses and angles α and β as discussed in section 3. By virtue of these relations, the numerical values of δS and δT in the MSSM are much smaller than 1. For example, by taking $m_{A^0} \gg m_Z$ and applying the various MSSM tree-level relations, one easily obtains the asymptotic results quoted in eqs. (33) and (34). Moreover, one can check that $\delta U \ll \delta S$, δT.

Acknowledgments

I would like to express my deep appreciation to my collaborators Marco Diaz and Ralf Hempfling whose contributions to the work on radiatively corrected Higgs masses were instrumental to the development of the material reported in this paper. I am also grateful to Yosef Nir for his part of the $h^0A^0A^0$ project. In addition, I thank Fabio Zwirner for his contributions to the work that produced figs. 1 and 2. Finally, conversations with Dallas Kennedy and Michael Peskin concerning S, T and U are gratefully acknowledged. This work was supported in part by the U.S. Department of Energy.

REFERENCES

1. J.F. Gunion, H.E. Haber, G. Kane and S. Dawson, *The Higgs Hunter's Guide* (Addison-Wesley Publishing Company, Reading, MA, 1990).
2. H.E. Haber, in *Testing the Standard Model,* Proceedings of the 1990 Theoretical Advanced Study Institute in Elementary Particle Physics, edited by M. Cvetič and P. Langacker (World Scientific, Singapore, 1991) p. 340.
3. G. 't Hooft, in *Recent Developments in Gauge Theories,* Proceedings of the NATO Advanced Summer Institute, Cargese, 1979, edited by G. 't Hooft *et al.* (Plenum, New York, 1980) p. 135.
4. L. Susskind, *Phys. Rep.* **104** (1984) 181.
5. E. Witten, *Nucl. Phys.* **B188** (1981) 513; S. Dimopoulos and H. Georgi, *Nucl. Phys.* **B193** (1981) 150; N. Sakai, *Z. Phys.* **C11** (1981) 153; R.K. Kaul, *Phys. Lett.* **109B** (1982) 19.
6. H.P. Nilles, *Phys. Rep.* **110** (1984) 1; H.E. Haber and G.L. Kane, *Phys. Rep.* **117** (1985) 75; A.B. Lahanas and D.V. Nanopoulos, *Phys. Rep.* **145** (1987) 1; R. Barbieri, *Riv. Nuovo Cimento* **11** (1988) 1.
7. H.E. Haber, to appear in the *Proceedings of the 1992 Theoretical Advanced Study Institute in Elementary Particle Physics* , Boulder, CO, 1–26 June 1992, SCIPP preprint (1992).
8. For a comprehensive review and a complete set of references, see Chapter 4 of ref. 1.
9. H.E. Haber and Y. Nir, *Nucl. Phys.* **B335** (1990) 363.
10. J.M. Cornwall, D.N. Levin and G. Tiktopoulos, *Phys. Rev. Lett.* **30** (1973) 1268; *Phys. Rev.* **D10** (1974) 1145; C.H. Llewellyn Smith, *Phys. Lett.* **46B** (1973) 233; H.A. Weldon, *Phys. Rev.* **D30** (1984) 1547; J.F. Gunion, H.E. Haber and J. Wudka, *Phys. Rev.* **D43** (1991) 904.
11. S. Glashow and S. Weinberg, *Phys. Rev.* **D15** (1977) 1958.

12. K. Hisaka *et al.* [Particle Data Group], *Phys. Rev.* **D45** (1992) S1.
13. D. Decamp *et al.* [ALEPH Collaboration], *Phys. Lett.* **B237** (1990) 291; P. Abreu *et al.* [DELPHI Collaboration], *Phys. Lett.* **B245** (1990) 276; *Nucl. Phys.* **B373** (1992) 3; B. Adeva *et al.* [L3 Collaboration], *Phys. Lett.* **B251** (1990) 311; M.Z. Akrawy *et al.* [OPAL Collaboration], *Z. Phys.* **C49** (1991) 1; P.D. Acton *et al.*, *Phys. Lett.* **B268** (1991) 122.
14. D. Decamp *et al.* [ALEPH Collaboration], *Phys. Lett.* **B265** (1991) 475; D. Buskulic *et al.* [ALEPH Collaboration], *Phys. Lett.* **B285** (1992) 309.
15. R. Hempfling, preprint SCIPP 92/12 (1992), to be published in *Phys. Lett. B.*
16. V. Barger, J.L. Hewett and R.J.N. Phillips, *Phys. Rev.* **D41** (1990) 3421.
17. J. Bagger, S. Dimopoulos and E. Masso, *Phys. Lett.* **156B** (1985) 357; *Phys. Rev. Lett.* **55**(1985) 920.
18. G.M. Asatryan, A.N. Ioannisyan and S.G. Matinyan, *Sov. J. Nucl. Phys.* **53** (1991) 371 [*Yad. Fiz.* **53**, (1991) 592]; M. Carena, T.E. Clark, C.E.M. Wagner, W.A. Bardeen and K. Sasaki, *Nucl. Phys.* **D369** (1992) 33.
19. H.E. Haber and F. Zwirner, unpublished.
20. F. Abe *et al.* [CDF Collaboration], *Phys. Rev. Lett.* **68** (1992) 447.
21. See *e.g.*, G.F. Giudice and G. Ridolfi, *Z. Phys.* **C41** (1988) 447; M. Olechowski and S. Pokorski, *Phys. Lett.* **B214** (1988) 393; M. Drees and M.M. Nojiri, *Nucl. Phys.* **B369** (1992) 54.
22. T. Appelquist and J. Carazzone, *Phys. Rev.* **D11** (1975) 2856; B. Ovrut and H. Schnitzer, *Phys. Rev.* **D22** (1980) 2518; Y. Kazama and Y.-P. Yao, *Phys. Rev.* **D25** (1982) 1605; J.C. Collins, *Renormalization* (Cambridge University Press, Cambridge, 1984), Chapter 8.
23. M. Veltman, *Nucl. Phys.* **B123** (1977) 89; M.B. Einhorn, D.R.T. Jones, and M. Veltman, *Nucl. Phys.* **B191** (1981) 146.
24. J.C. Collins, F. Wilczek and A. Zee, *Phys. Rev.* **D18** (1978) 242.
25. D. Toussaint, *Phys. Rev.* **D18** (1978) 1626.
26. M. Chanowitz, M. Furman and I. Hinchliffe, *Phys. Lett.* **78B** (1978) 285; *Nucl. Phys.* **B153** (1979) 402.
27. W.J. Marciano and A. Sirlin, *Phys. Rev.* **D22** (1980) 2695 [E: **D31** (1985) 213].
28. G. Altarelli, R. Barbieri, and S. Jadach, *Nucl. Phys.* **B369** (1992) 3 [E: **B376** (1992) 444].
29. P. Langacker and M. Luo, *Phys. Rev.* **D44** (1991) 817; J. Ellis, G.L. Fogli and E. Lisi, *Phys. Lett.* **B274** (1992) 456; The LEP Collaborations: ALEPH, DELPHI, L3, and OPAL, *Phys. Lett.* **B276** (1992) 247; D. Schaile, *Z. Phys.* **C54** (1992) 387; P. Renton, Oxford preprint OUNP-91-30 (1991).

30. P. Langacker, U. Penn preprint UPR-0492T (1992), invited talk presented at the International Workshop on Electroweak Physics Beyond the Standard Model, Valencia, Spain, September, 1991.
31. M. Veltman, *Acta Phys. Pol.* **B8** (1977) 475; M.B. Einhorn and J. Wudka, *Phys. Rev.* **D39** (1989) 2758.
32. B.W. Lynn, M.E. Peskin and R.G. Stuart, in *Physics at LEP*, edited by J. Ellis and R. Peccei, CERN Yellow Report CERN-86-02 (1986) p. 90; B. Lynn and D.C. Kennedy, *Nucl. Phys.* **B321** (1989) 83; **B322** (1989) 1; D.C. Kennedy, *Nucl. Phys.* **B351** (1991) 81; M.E. Peskin, in *Physics at the 100 GeV Mass Scale*, Proceedings of the 1989 SLAC Summer Institute, edited by E.C. Brennan, SLAC-Report-361 (1990) p. 71.
33. M.E. Peskin and T. Takeuchi, *Phys. Rev. Lett.* **65** (1990) 964; *Phys. Rev.* **D46** (1992) 381.
34. G. Altarelli and R. Barbieri, *Phys. Lett.* **B253** (1990) 161.
35. W.J. Marciano and J.L. Rosner, *Phys. Rev. Lett.* **65** (1990) 2963; D.C. Kennedy and P. Langacker, *Phys. Rev. Lett.* **65** (1990) 2967 [E: **66** (1991) 395]; *Phys. Rev.* **D44** (1991) 1591; D.C. Kennedy, *Phys. Lett.*, **B268** (1991) 86; J.Ellis, G.L. Fogli, and E. Lisi, *Phys. Lett.* **B285** (1992) 238.
36. D.C. Kennedy, in *Perspectives in the Standard Model*, Proceedings of the 1991 Theoretical Advanced Study Institute in Elementary Particle Physics, Boulder, CO, 3-28 June 1991, edited by R.K. Ellis, C.T. Hill, and J.D. Lykken (World Scientific, Singapore, 1992) p. 163.
37. R. Barbieri, M. Frigeni, F. Giuliani and H.E. Haber, *Nucl. Phys.* **B341** (1990) 309; M. Drees and K. Hagiwara, *Phys. Rev.* **D42** (1990) 1709; P. Gosdzinsky and J. Sola, *Phys. Lett.* **B254** (1991) 139; *Mod. Phys. Lett.* **A6** (1991) 1943; M. Drees, K. Hagiwara, and A. Yamada, *Phys. Rev.* **D45** (1992) 1725; R. Barbieri, M. Frigeni and F. Caravaglios, *Phys. Lett.* **B279** (1992) 169.
38. H.E. Haber, SCIPP preprint in preparation.
39. S. Bertolini, *Nucl. Phys.* **B272** (1986) 77.
40. R.S. Lytel, *Phys. Rev.* **D22** (1980) 505; J.-M. Frère and J.A.M. Vermaseren, *Z. Phys.* **C19** (1983) 63; W. Hollik, *Z. Phys.* **C32** (1986) 291; **C37** (1988) 569.
41. C.D. Froggatt, R.G. Moorhouse, and I.G. Knowles, *Phys. Rev.* **D45** (1992) 2471; ANL-HEP-PR-92-01 (1992); T. Inami, C.S. Lim and A. Yamada, YITP/K-951 (1991).
42. G. Altarelli and P. Franzini, *Z. Phys.* **C37** (1988) 271; G.G. Athanasiu, P.J. Franzini and F.J. Gilman, *Phys. Rev.* **D32** (1985) 3010; S.L. Glashow and E.E. Jenkins, *Phys. Lett.* **B196** (1987) 233; F. Hoogeveen and C.N. Leung,

Phys. Rev. **D37** (1988) 3340; J.F. Gunion and B. Grzadkowski, *Phys. Lett.* **B243** (1990) 301.

43. C.Q. Geng and J.N. Ng, *Phys. Rev.* **D38** (1988) 2857.
44. S. Bertolini, F. Borzumati, A. Masiero and G. Ridolfi, *Nucl. Phys.* **B353** (1991) 591.
45. A. Buras, P. Krawczyk, M.E. Lautenbacher and C. Salazar, *Nucl. Phys.* **B337** (1990) 284.
46. A. Djouadi, G. Girardi, C. Verzegnassi, W. Hollik and F.M. Renard, *Nucl. Phys.* **B349** (1991) 48; M. Boulware and D. Finnell, *Phys. Rev.* **D44** (1991) 2054.
47. W.-S. Hou and R.S. Willey, *Phys. Lett.* **B202** (1988) 591; *Nucl. Phys.* **B326** (1989) 54; T. Rizzo, *Phys. Rev.* **D38** (1988) 820; X.-G. He, T.D. Nguyen and R.R. Volkas, *Phys. Rev.* **D38** (1988) 814; M. Ciuchini, *Mod. Phys. Lett.* **A4** (1989) 1945.
48. Z. Kunszt and W.J. Stirling, *Phys. Lett.* **B242** (1990) 507; N. Brown, *Z. Phys.* **C49** (1991) 657; V. Barger, R.J.N. Phillips and K. Whisnant, *Phys. Rev.* **D43** (1991) 1110; D.J. Summers, *Phys. Lett.* **B274** (1992) 209.
49. H.E. Haber and R. Hempfling, *Phys. Rev. Lett.* **66** (1991) 1815.
50. Y. Okada, M. Yamaguchi and T. Yanagida, *Prog. Theor. Phys.* **85** (1991) 1; *Phys. Lett.* **B262** (1991) 54; J. Ellis, G. Ridolfi and F. Zwirner, *Phys. Lett.* **B257** (1991) 83; **B262** (1991) 477; R. Barbieri, M. Frigeni, and F. Caravaglios, *Phys. Lett.* **B258** (1991) 167.
51. R. Barbieri and M. Frigeni, *Phys. Lett.* **B258** (1991) 395; A. Yamada, *Phys. Lett.* **B263** (1991) 233.
52. J.R. Espinosa and M. Quiros, *Phys. Lett.* **B267** (1991) 27.
53. P.H. Chankowski, S. Pokorski and J. Rosiek, *Phys. Lett.* **B274** (1992) 191; **B281** (1992) 100.
54. H.E. Haber and R. Hempfling, SCIPP 91/33 (1992).
55. D.M. Pierce, A. Papadopoulos, and S. Johnson, *Phys. Rev. Lett.* **68** (1992) 3678.
56. K. Sasaki, M. Carena and C.E.M. Wagner, MPI-Ph/91-109 (1991).
57. A. Brignole, *Phys. Lett.* **B281** (1992) 284.
58. M.A. Diaz and H.E. Haber, SCIPP 91/13 (1992), *Phys. Rev.* **D46** (1992) in press.
59. M.A. Diaz and H.E. Haber, *Phys. Rev.* **D45** (1992) 4246.
60. J.F. Gunion and A. Turski, *Phys. Rev.* **D39** (1989) 2701; **D40** (1989) 2333.
61. A. Brignole, J. Ellis, G. Ridolfi and F. Zwirner, *Phys. Lett.* **B271** (1991) 123; [E: **B273** (1991) 550].

62. A. Brignole, *Phys. Lett.* **B277** (1992) 313.
63. T.P. Cheng, E. Eichten and L.-F. Li, *Phys. Rev.* **D9** (1974) 2259.
64. N. Cabibbo, L. Maiani, G. Parisi, R. Petronzio *Nucl. Phys.* **B158** (1979) 295.
65. S. Rudaz and J. Ellis, *Phys. Lett.* **128B** (1983) 248.
66. S. Coleman and E. Weinberg, *Phys. Rev.* **D7** (1973) 1888.
67. See section 2.5 of ref. 1.
68. E. Franco and A. Morelli, *Nuovo Cim.* **96A** (1986) 257.
69. J.M. Frère, D.R.T. Jones and S. Raby, *Nucl. Phys.* **B222** (1983) 11; M. Claudson, L.J. Hall and I. Hinchliffe, *Nucl. Phys.* **B228** (1983) 501; J.-P. Derendinger and C.A. Savoy, *Nucl. Phys.* **B237** (1984) 307; J.F. Gunion, H.E. Haber and M. Sher, *Nucl. Phys.* **B306** (1988) 1; H. Komatsu, *Phys. Lett.* **B154** (1988) 323.
70. J.F. Gunion, contribution to this volume.
71. H.E. Haber, R. Hempfling and Y. Nir, SCIPP 91/40 and WIS-92/5/Feb-PH (1992), *Phys. Rev.* **D46** (1992) in press.
72. J.F. Gunion, R. Bork, H.E. Haber and A. Seiden, UCD-91-29 and SCIPP 91/34 (1991), *Phys. Rev.* **D46** in press; J.F. Gunion, H.E. Haber and C. Kao, UCD-91-32 and SCIPP 91/44 (1991), *Phys. Rev.* **D46** (1992) in press; V. Barger, M.S. Berger, A.L. Stange, and R.J.N. Phillips, *Phys. Rev.* **D45** (1991) 4128; Z. Kunszt and F. Zwirner, CERN-TH.6150/91 and ETH-TH/91-7 (1991); A. Yamada, preprint UT-Komaba 92-1 (1992).
73. H.E. Haber, SCIPP 92/10 (1992), to appear in *Proceedings of the Workshop on Future e^+e^- Linear Colliders*, Saariselkä, Finland, 9–14 September 1991.
74. T.P. Cheng, E. Eichten and L.-F. Li, *Phys. Rev.* **D9** (1974) 2259; K. Inoue, A. Kakuto, and Y. Nakano, *Prog. Theor. Phys.* **63** (1980) 234; H. Komatsu, *Prog. Theor. Phys.* **67** (1982) 1177; K. Inoue, A. Kakuto, H. Komatsu and S. Takeshita, *Prog. Theor. Phys.* **67** (1982) 1889; **68** (1982) 927 [E: **70** (1983) 330] **71** (1984) 413; C. Hill, C.N. Leung and S. Rao, *Nucl. Phys.* **B262** (1985) 517.
75. G. Passarino and M. Veltman, *Nucl. Phys.* **B160** (1979) 151.
76. J.D. Bjorken and S.D. Drell, *Relativistic Quantum Mechanics* (McGraw-Hill, New York, 1964).